Analyzing the degradation of roadside infrastructure

by

Luke Strand Augustine

B.S., Kansas State University, 2017

A THESIS

submitted in partial fulfillment of the requirements for the degree

MASTER OF SCIENCE

Department of Civil Engineering
College of Engineering

KANSAS STATE UNIVERSITY
Manhattan, Kansas

2019

Approved by:

Major Professor
Dr. Stacey Kulesza

Copyright

Abstract

Metals are used in a variety of different ways to strengthen and enhance transportation infrastructure. Steel, one of the most commonly used metals, can be found as strips in MSE walls and corrugated metal pipes running underneath roads and highways. These elements are often galvanized or coated with another material in an effort to protect and increase the service life. Having the ability to assess the present state of metals in infrastructure is important when projecting rehabilitation or replacement.

The objectives of this research were twofold. The first was to observe the current state of corrugated metal pipe in Kansas. This work was done as a follow up to two previous studies conducted by the Kansas Department of Transportation that examined the effects of a policy change in 1975 that allowed for lighter gauge corrugated metal pipe to be used in their projects. The results from these studies were compared with those found in this research and were consistent with the conclusion that the policy change led to a shorter service life expectancy for pipes installed after 1975. A reversion to pre-1975 policy corrected that problem, validated by the current study. Additional characteristics investigated with regards to the deterioration rate of the corrugated metal pipes included material type, corrugation dimensions, resistivity, and chloride concentration in the surrounding soil.

The second objective was to evaluate the corrosive environments of aggregate backfill in MSE walls. This work was done as an exploration of a unique application of electrical resistivity where measurements were taken into a vertical plane (into the backfill of a mechanically stabilized earth wall directly behind the panels of the wall) instead of a horizontal plane (typically the ground). Five mechanically stabilized earth walls in total were analyzed by taking into-the-wall measurements at the base. Three walls were selected to take electrical resistivity

surveys at the top of the wall and the backfill of four walls was classified. These results support the potential of using a modified four-electrode electrical resistivity measurement to identify corrosive environments in MSE walls.

Table of Contents

List of Figures

List of Tables

Acknowledgements

I first want to thank my major professor, Dr. Stacey Kulesza for her assistance and guidance throughout this project and my entire academic career at Kansas State University. Her mentorship through my undergraduate and graduate degrees has prepared me to be successful in my professional endeavors.

I also want to thank my committee members, Dr. Prathap Parameswaran and Dr. Christopher Jones, for their support. Additionally, I want to thank my peers, Weston Koehn, Zahidul Karim, Mark Mathis, Robert Sherwood, Saikat Kuili, and Arvind Kannan, for their assistance and expertise with laboratory and field testing. Their help is greatly appreciated.

Finally, I want to thank the Kansas Department of Transportation for their financial sponsorship of both projects.

Chapter 1 - Introduction

Metal components are a common part of transportation infrastructure. They can be used as reinforcement (e.g., in pavement, mechanically stabilized earth (MSE) walls) or as infrastructure (e.g., steel H-piles, corrugated metal pipe (CMP)). With the use of metals comes the problem of corrosion. Nationally, the estimated direct cost of corrosion is 3.1% of the Gross Domestic Product (GDP) (Kutz, 2005). Direct costs include the price of replacement material and labor for installation, among others. The estimated indirect cost of corrosion is approximately the same as the direct cost at 3.1% of GDP. Indirect costs include the cost of lost productivity due to failure, delay, and litigation as well as the cost of non-operator/owner activities. The combined direct and indirect costs of corrosion are 6.2% of the GDP. Therefore, corrosion in transportation infrastructure is costly. Two examples of corrosion assessment by the Kansas Department of Transportation (KDOT) are corrosion of CMP in Kansas (Stratton et al., 1990 & Crowder, 2017) and the corrosion potential of MSE wall backfill (Tucker-Kulesza et al., 2016). Although there are many transportation infrastructure elements where corrosion is of concern, this thesis focuses on CMP and MSE wall corrosion.

Corrugated metal pipes have been used for decades as a means to transport stormwater from one side of the road to the other. Traditionally, CMP are made of galvanized steel. In 1989, KDOT began a study on CMP in response to a policy change enacted in 1975 allowing for a lighter gauge CMP. KDOT wanted to examine whether or not there was a change in the rate of corrosion of CMP installed before and after the policy change. Stratton (1989) found that there was indeed an adverse change in the rate of corrosion for those CMP installed after 1975. In other words, the CMP installed after 1975 was corroding at a much faster rate than those installed before 1975. These findings prompted a follow up study. Stratton et al. (1990)

evaluated a much larger number of CMP across the state and were able to substantiate Stratton (1989) conclusions. KDOT ultimately reverted back to their pre-1975 policies on CMP gauge based on these studies. KDOT was interested in reevaluating CMP corrosion through this research due to the addition of aluminum and aluminized CMP alongside tradition galvanized CMP and to validate the 1975 policy reversion.

KDOT is also interested in the corrosion of metallic MSE wall reinforcement. MSE walls were first utilized in the United States during the 1970s (Armour et al., 2004). In Kansas, KDOT commonly uses MSE walls in overpasses and interchanges throughout the highway system. MSE walls are effective structures for supporting earth necessary to elevate roads because of their minimal footprint and increased strength relative to other options. A typical cross section can be found in Fig. 1.1. They are comprised of a wall face that is typically modular panels or blocks, standardized aggregate backfill most commonly sand or gravel, and soil reinforcement that can be metal strips or geosynthetics (Elias et al., 2009). The facing elements are supported by a leveling pad and natural soil can be present behind the standard backfill if the wall is constructed in front of an existing slope.

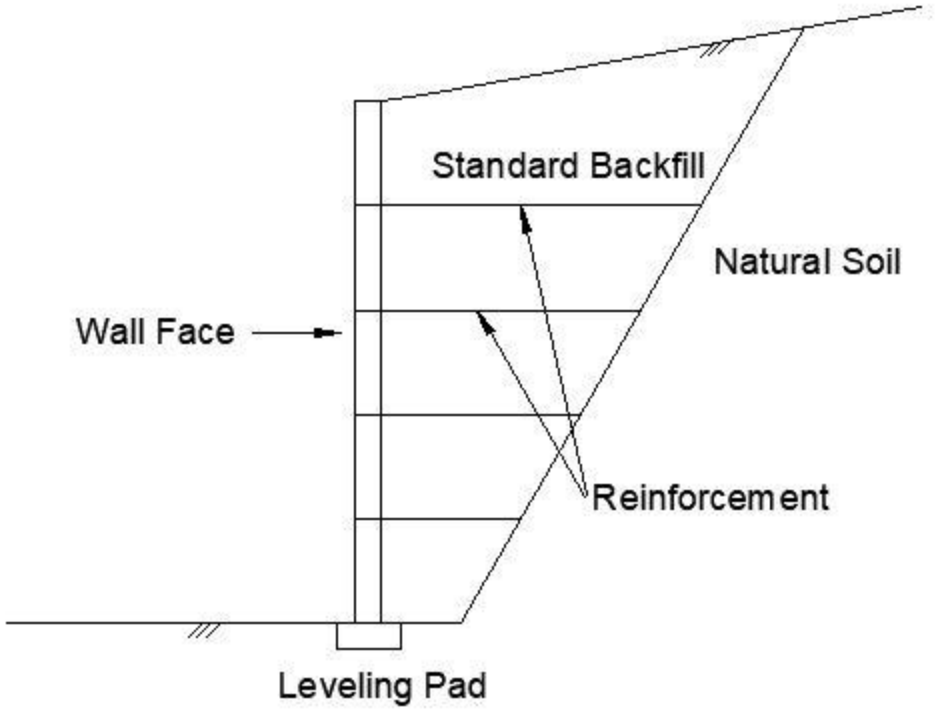

Fig. 1.1 Typical MSE wall cross section

MSE wall backfill is selected based a number of specifications, including electrical resistivity, pH, concentration of chlorides, sulfates, and organic content, and grain size distribution (Hansen, 2015 & Elias et al., 2009). The electrical resistivity is commonly used to estimate the corrosion potential of the backfill (Snapp et al., 2017). To estimate the corrosion potential of MSE wall backfill, DOTs utilize electrical resistivity through AASHTO method T 288-12 (2012c) and ASTM standards G187-12 (2012c) and G57-06 (2012a); KDOT uses AASHTO method T 288-12. All methods use variations of soil boxes to measure the electrical resistivity of a soil sample in a laboratory. All of these methods are measured in the laboratory, however, and not *in situ* measurements which may more accurately represent field conditions. They are also only performed as a means of quality assurance prior to construction and are not performed throughout the service life of the MSE wall.

Currently, the only method widely used to assess backfill during the service life of an MSE wall is through the use of buried metallic coupons (Elias et al., 2009). These coupons are used to evaluate the corrosiveness of the backfill environment. Using coupons can be challenging because it requires accurate and easily accessible records and conducting a corrosion monitoring schedule. The lack of evaluation methods has generated a need for alternative *in situ* methods.

The benefit of using electrical resistivity is that it is dependent on a number of soil properties (i.e., degree of saturation, degree of compaction, and presence of salts or other dissolved ions) (Everett, 2013). The way electrical resistivity is measured—in a laboratory setting using only a small soil sample for MSE walls or as a point measurement in the field for CMP—raises concerns because of the assumption that the soil is homogeneous around the metallic element, which is not always the case. Additionally, with laboratory measurements, *in situ* conditions can be difficult to replicate and negatively affect the accuracy of the data. However, electrical resistivity could be an effective measurement *in situ*.

With KDOT placing significance on the research of corrosion of roadside metallic elements, the objectives of this research were to twofold. The first was to investigate the corrosion of CMP in Kansas. Measured properties of the CMP and surrounding soil were material type, corrugation dimensions, electrical resistivity, and chloride concentration. These properties were analyzed alongside the deterioration rate and policy changes affecting CMP in order to gain an understanding of the causes of their corrosion. As a part of this objective, the effectiveness of electrical resistivity to predict the service life of CMP was also evaluated.

The second objective was to develop an experimental methodology to evaluate the corrosive environments surrounding MSE wall reinforcement using electrical resistivity *in situ*.

This method was conducted by using a series of four point electrical resistivity arrays placed directly into the backfill of the MSE wall, through the wall panels. This method was assessed in conjunction with electrical resistivity surveys taken at the top of the wall and grain size distribution determined in the laboratory.

This thesis is divided into five chapters. Following this introduction is a literature review, in Chapter 2, that describes the process of corrosion and studies in other states involving the corrosion of CMP and MSE wall reinforcement. Chapter 3 establishes the methodology used for both components of this research. Chapter 4 presents the results gathered accompanied by a discussion of the results. Chapter 5 establishes conclusions of the research and future work considerations. Following the conclusions are the references and Appendices. The appendices include the full set of collected data for the CMP in this study and the characteristics of the MSE walls examined.

Chapter 2 - Literature Review

2.1 Corrosion

Corrosion is "the chemical or electrochemical reaction between a material, usually a metal, and its environment that produces a deterioration of the material and its properties" (ASTM 2012b). In metals, the material experiences loss of strength, ductility, and the material itself is consumed (Cicek, 2014). It is easily and most commonly observed as reddish-brown rust. The process of rust formation requires the presence of an anode, cathode, and electrolyte. The anode and cathode are determined based on their place in the galvanic series which is determined by nobility. In a system comprised of two different metals the metal that is less noble, or has a lower electrode potential, is the anode and the metal that is more noble is the cathode. In a system with only one metal, the anode is the area covered by the electrolytic solution and the cathode is uncovered. Common metals in the galvanic series are shown in Fig. 2.1. In CMP and other outdoor metals, the anodic region is commonly zinc or aluminum, the cathodic region is most commonly iron or steel, and the electrolytic solution is water.

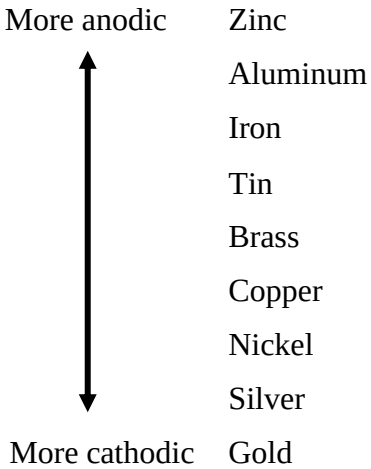

Fig. 2.1 Galvanic series of common metals

The formation of rust on iron requires iron, water, and oxygen to form iron (III) oxide (Ahmad, 2016). The iron works as both the anode and the cathode. It begins with the adsorption of water onto the surface of the metal followed by the dissolution of iron into the water. The reaction is shown in Equation 2.1.

$$2Fe \rightarrow 2Fe^{2+} + 4e^{-} \tag{2.1}$$

Following the release of the electrons from the iron is a reduction of oxygen dissolved into water. This reaction is shown in Equation 2.2.

$$O_2 + 2H_2O + 4e^{-} \rightarrow 4OH^{-} \tag{2.2}$$

The production of hydroxide and iron molecules react to form iron hydroxide, shown in Equation 2.3.

$$2Fe^{2+} + 4OH^{-} \rightarrow 2Fe(OH)_2 \tag{2.3}$$

The iron hydroxide then reacts with oxygen to create iron (III) oxide, shown in Equation 2.4, which is the visible reddish-brown rust.

$$4Fe(OH)_2 \rightarrow 2Fe_2O_3 \cdot H_2O + 2H_2O \tag{2.4}$$

There are two main types of corrosion: uniform and non-uniform corrosion (Cicek, 2014). Uniform corrosion occurs when corrosion is evenly distributed over the surface of the metal. The loss of thickness in the metal is relatively shallow when compared to non-uniform corrosion. Uniform corrosion is commonly attributed to atmospheric corrosion, corrosion in water, and soil corrosion, all of which require consistent coverage of the metal (Cicek, 2014). Fig. 2.2 shows the beginning stages of atmospheric corrosion as the spelter, (i.e., the protective zinc coating) on this particular CMP is corroded.

Fig. 2.2 Loss of spelter in CMP US-56/9-yr

The second type of corrosion, non-uniform corrosion, is localized. The localization can cause perforations and significant material loss in small areas (Cicek, 2014). Common types of non-uniform corrosion are galvanic corrosion and pitting. An example of pitting can be seen in Fig. 2.3.

Fig. 2.3 Pitting corrosion in corrugated metal pipe

As mentioned in Chapter 1, corrosion has three requirements, an anode, a cathode, and electrolytic solution. These three components form a galvanic cell. In a galvanic cell, electrons are released at the anode and conducted to the cathode. The remaining ions from the anode are oxidized to form rust. A simple diagram of this process can be seen in Fig. 2.4.

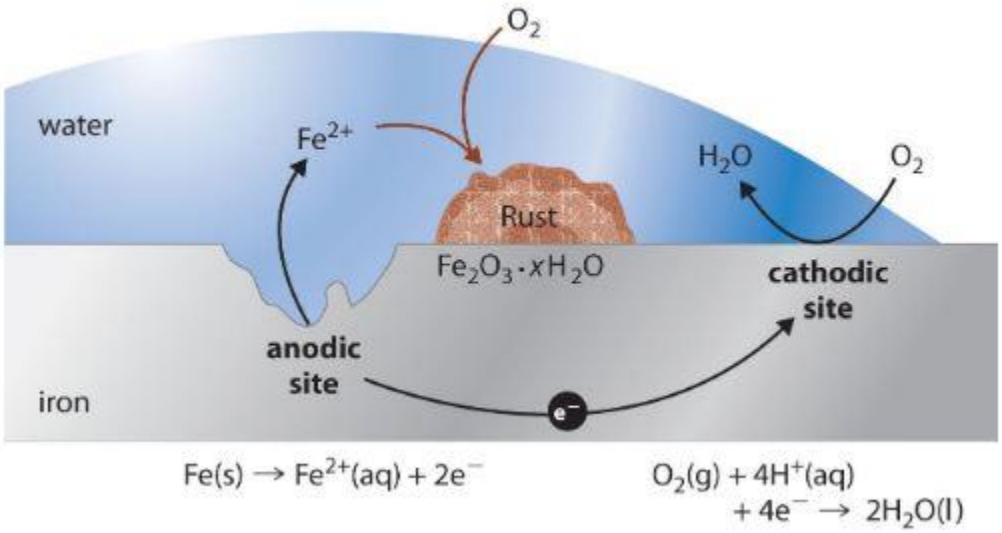

Fig. 2.4 Diagram of the corrosion process (Averill & Eldredge, 2012)

2.1.1 Identifying Corrosive Environments

There are a variety of ways to identify corrosive environments. Among some of the most common are resistivity and ion concentrations (Elias et al., 2009), which are described herein as they were the primary measurements used in this research.

2.1.1.1 Ion Concentrations

The presence of ions in saline water in roadside settings commonly occur in the winter months as a result of dissolved road deicers. Naturally occurring salt deposits can also effect the salinity of surface water (Sawin and Buchanan, 2002). In Kansas, naturally forming salt deposits in the central and south-central part of the state have increased the salinity of some surface water through natural and human-induced processes. The Smoky Hill River has naturally increased

salinity levels due to the migration of brine, containing naturally dissolved salts from the bedrock, to the river (Sawin and Buchanan, 2002). Groundwater in Reno and Rice counties have increased salinity levels due to early salt mining techniques that produced saltwater (Sawin and Buchanan, 2002). The pumping of groundwater can also bring saline water up to the surface and increase the salinity of surrounding surface water. The secondary maximum contaminant level (SMCL) of chloride, set by the Environmental Protection Agency (EPA), is 250 ppm and the total dissolved solids SMCL is 500 ppm (DeSimone et al., 2014). During winter months, studies of roadside soils have found sodium concentrations ranging from 352-513 ppm and chloride concentrations from 577-2353 ppm (Li et al., 2015). The wide range in concentrations is likely due to the varying amount of deicing salts a segment of road received during the winter months. Concentrations of these ions as a result of deicers have been found as far as 150 m from the roadside (Willmert et al., 2018). The amount of dissolved salts are directly proportional to the conductivity of the soil moisture. As salt concentrations, and consequently conductivity, increase, flow of corrosive currents is increased. Therefore, permissible levels of salts have been defined to reduce the likelihood of increased corrosion rates (Elias et al., 2009).

2.1.1.2 Electrical Resistivity

Electrical resistivity, ρ, is the opposition of the flow of electricity a soil or other material exhibits. It is inversely related to conductivity and can be calculated using Equation 2.5,

$$\rho = \frac{RA}{L} \tag{2.5}$$

where R is the resistance (Ohm), A is the cross-sectional area (m^2) the current flows through, and L is the distance (m) the current travels. Electrical resistivity is commonly accepted as an indicator for corrosive environments (Elias et al., 2009). Table 2.1 provides the series of electrical resistivity ranges characterizing very corrosive to non-corrosive environments in

transportation infrastructure. The National Bureau of Standards has shown that corrosion rates increase by approximately 25% in each successive corrosive range (Elias et al., 2009).

Table 2.1 Corrosive potential related to electrical resistivity measurements (Elias et al. 2009)

Aggressiveness	**Resistivity (Ohm-m)**
Very Corrosive	< 7
Corrosive	7 – 20
Moderately Corrosive	20 – 50
Mildly Corrosive	50 – 100
Non-corrosive	> 100

The electrical resistivity of a soil is influenced by many factors including pore space, pore-water saturation, ion concentration within the pore water, and temperature (ASTM, 2012a). Current can more easily flow in porous media, like soil, as pore-water saturation increases thus increasing conductivity and decreasing resistivity (Loke, 1999). As ion concentration increases, the pore-water has a greater ability to carry a charge, again increasing conductivity and decreasing resistivity (Elias et al., 2009). Temperature increases the activity of the ions within the pore-water, making them more susceptible to carrying a charge increasing conductivity and decreasing resistivity (ASTM, 2012a). Common electrical resistivity values of geo-materials can be found in Table 2.2.

Table 2.2 Common electrical resistivity values (Everett, 2013)

Material	**Resistivity (Ohm-m)**
Clay	1 – 20
Sand, wet to moist	20 – 200
Shale	1 – 500
Porous Limestone	100 – 1,000
Dense Limestone	1,000 – 1,000,000

In soil, electrical resistivity is typically measured using four electrodes. Two are designated for the inflow and outflow of electricity in the soil, commonly noted as A and B, and two are designated to measure the voltage potential, commonly noted as P and Q. Electrical resistivity can be measured in the lab using ASTM G57 (2012a) or with an automated data acquisition system. With an automated system, hundreds of data points can be collected rapidly and used to generate a 2-D or 3-D image. These images are created with measured apparent resistivity. Apparent resistivity, ρ_a, is measured assuming the surrounding soil is homogenous and is calculated using Equation 2.6,

$$\rho_a = \frac{V}{I} * k \tag{2.6}$$

where V is the measured voltage, I is the induced current, and k is the shape factor which is dependent on the array type.

Array Types

There are several four electrode array types that are commonly used to measure electrical resistivity and image the subsurface. Each test has different electrode configurations, resulting in different sensitivities and resolutions. Depth of investigation and objective of the survey should be considered when determining the proper array to use (Loke, 1999).

Schlumberger Array

The Schlumberger array was originally developed as a vertical sounding method for the oil industry. It is most effective at detecting horizontal layers in the subsurface. The array also has a high depth of investigation. The disadvantage of using the Schlumberger array is that it is poor at detecting changes along a horizontal layer (Everett, 2013). In other words, it does not detect vertical layers well. The configuration of the Schlumberger array, shown in Fig. 2.5, places voltage electrodes P and Q at a distance a from the center of the array. Current electrodes

A and B are placed outside of the voltage electrode pair at a distance of *na* from the center of the array. The shape factor *k* for the Schlumberger array is

$$k = \frac{1}{2}(n-1)(n+1)\pi a \tag{2.8}$$

where *a* is half of the distance between voltage electrode P and voltage electrode Q and *n* is the multiple of distance *a* that current electrode A or current electrode B is from the center of the array.

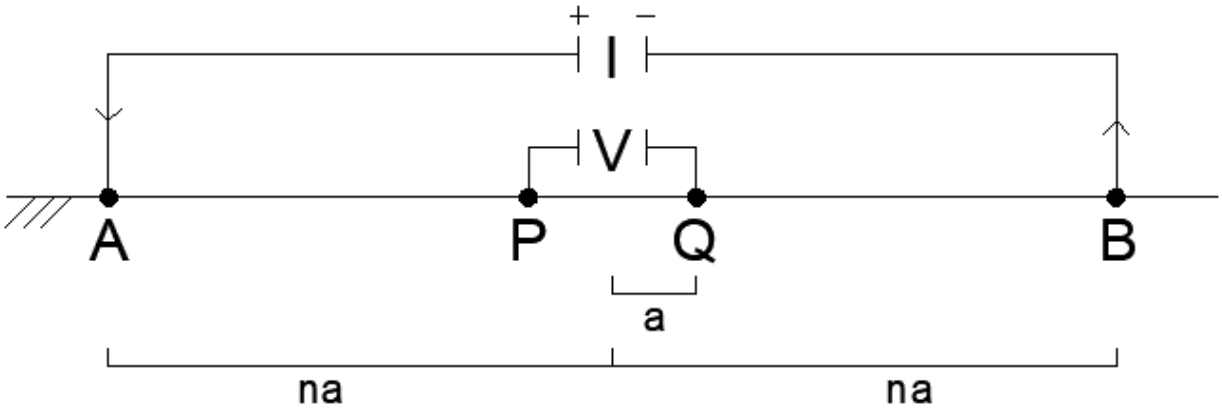

Fig. 2.5 Schlumberger array configuration

Wenner Array

The Wenner array is a popular array type because of the standardized test specified in ASTM G57 (ASTM, 2012a). This array was designed for use at a constant depth for lateral profiling of the subsurface. Opposite of the Schlumberger array, the Wenner array is not effective at detecting horizontal layers but is more effective at detecting vertical structures (Everett, 2013). It has a lesser depth investigation due to its configuration requirements. The configuration of the Wenner array, shown in Fig. 2.6, places voltage electrodes P and Q at a distance 0.5*a* from the center of the array. Current electrodes A and B are placed outside of the voltage electrode pair at a distance *a* from the voltage electrodes. The spacing between each electrode is identical. The shape factor *k* for the Wenner array is

$$k = 2\pi a \tag{2.9}$$

where *a* is the distance between each electrode.

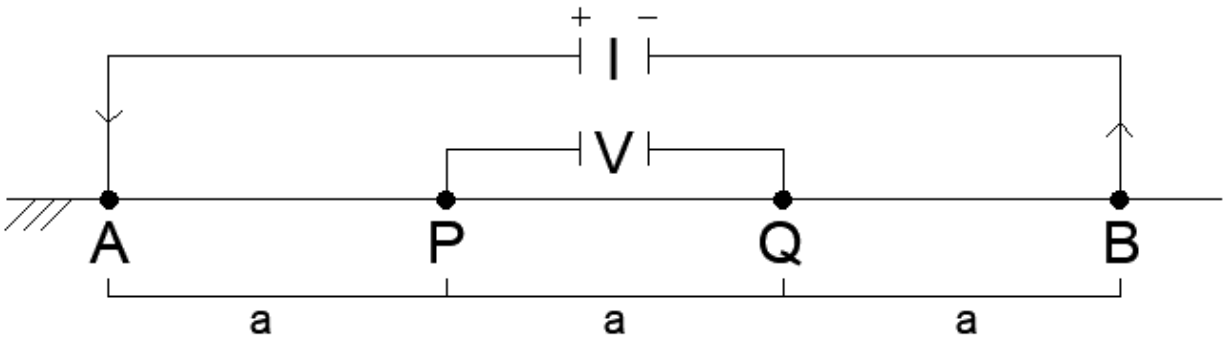

Fig. 2.6 Wenner array configuration

Dipole-Dipole Array

The Dipole-Dipole array is a widely used array type that has the advantage of vertical sounding of the Schlumberger array and the lateral profiling of the Wenner array (Everett, 2013). The disadvantage of the Dipole-Dipole array is its low sensitivity at the surface and shallower depth of investigation compared to the Wenner array (Loke, 1999). The configuration of the Dipole-Dipole array, shown in Fig. 2.7, places the voltage electrode pair opposite of the current electrode pair. Voltage electrode P and voltage electrode Q are separated by distance *a*, as are current electrode A and current electrode B. The distance between voltage electrode Q and current electrode A is *na*. The shape factor *k* for the Dipole-Dipole array is

$$k = \pi a n(n+1)(n+2) \tag{2.7}$$

where *a* is the distance between current electrode A and current electrode B and the distance between voltage electrode P and voltage electrode Q and *n* is the multiple of distance *a* that the electrode pairs are placed from each other.

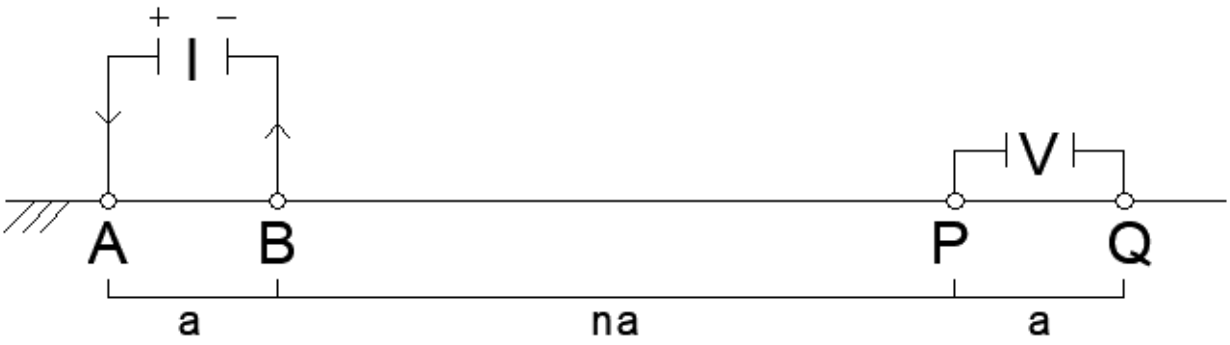

Fig. 2.7 Dipole-Dipole array configuration

For this research, the Schlumberger and Dipole-Dipole arrays were used because of their strength in imaging horizontal layers. This was an important characteristic because the conditions at the bottom of the MSE walls were of primary interest.

Depth of Investigation

The depth of investigation of electrical resistivity refers to the depth at which the measurement is taken. It is dependent on the survey type, electrode spacing, and spacing of the electrode pairs. Hallof (1957) established that the depth of investigation is at the intersection of two 45 degree lines stemming from the center of each electrode pair, as shown in Fig. 2.8.

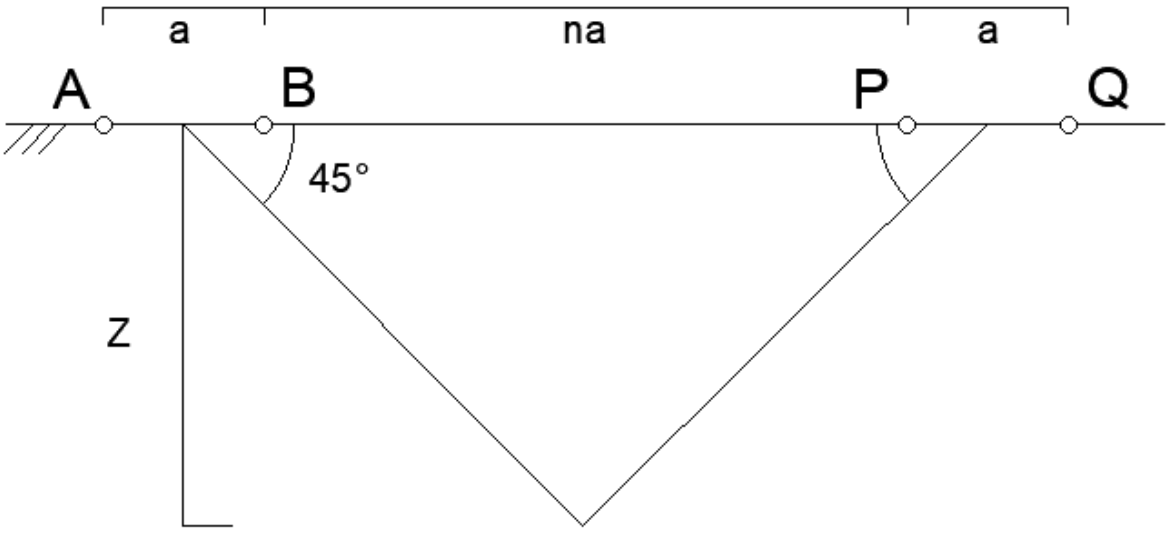

Fig. 2.8 Depth of investigation

Later, the depth of investigation was modified in an effort to more accurately plot resistivity measurements in the subsurface. Edwards (1977) identified that the resulting electrical resistivity data are of higher quality (i.e., less noise) when the assumed depth of investigation is such that half of the electrical resistivity signal is above and half of the electrical resistivity signal is below a point. Using this principle, Edwards (1977) defined,

$$n(n+1)(n+2)\{[n^2+u]^{-\frac{1}{2}} - 2[(n+1)^2+u]^{-\frac{1}{2}} + [\left(n+2)^2+u\right]^{-\frac{1}{2}}\right\} = 1 \quad (2.10)$$

where *n* is the multiple of distance *a* that the electrode pairs are placed from each other and *u* is defined in Equation 2.11,

$$u = 4(z/a)^2 \quad (2.11)$$

where *a* is the distance between current electrode A and current electrode B and the distance between voltage electrode P and voltage electrode Q and *z* is the depth of investigation. To compare, the depth of investigation of a four point Dipole-Dipole survey with n = 1 m and a = 1.5 m using Hallof (1957) would be 1.5 m. Using Edwards (1977) with the same n and a values, the depth of investigation would be 0.62 m.

Considering the depth of investigation is important for this research because of the limited volume of specified backfill behind the MSE wall face. If the depth of investigation was too deep (i.e., too far back into the backfill) the resistivity measurements would be influenced partially by the native soil behind the backfill. Ensuring that the depth of investigation did not reach past the specified backfill ensured that the resistivity measurements were representative only of the backfill and not the native soil.

Electrical Resistivity Probe

In addition to the various four point arrays discussed previously are single probe devices, such as a Collins Rod. Collins Rods have been used in the corrosion engineering field for over

40 years (Vilda, 2009). A Collins Rod is a hollow, hexagonal, steel rod designed to be pushed into the ground and measure the resistivity at a desired depth. The tip is conical in shape and is separated from the shaft by a thin spacer. Wires connect the tip to the resistivity meter and the hollow rod to the resistivity meter. The Collins Rod uses two-electrode linear polarization resistance technology to measure electrical resistivity (Vilda, 2009). The electrical resistivity is measurement is obtained by nulling the alternating current measurements between the tip and rod of the apparatus. Fig. 2.9 shows the configuration of a Collins Rod. With correct configuration, soil resistivity and a corrosion rate can be obtained with a single measurement (Vilda, 2009). The Collins Rod was used for this research in order to obtain a simple resistivity measurement of the soil surrounding CMP.

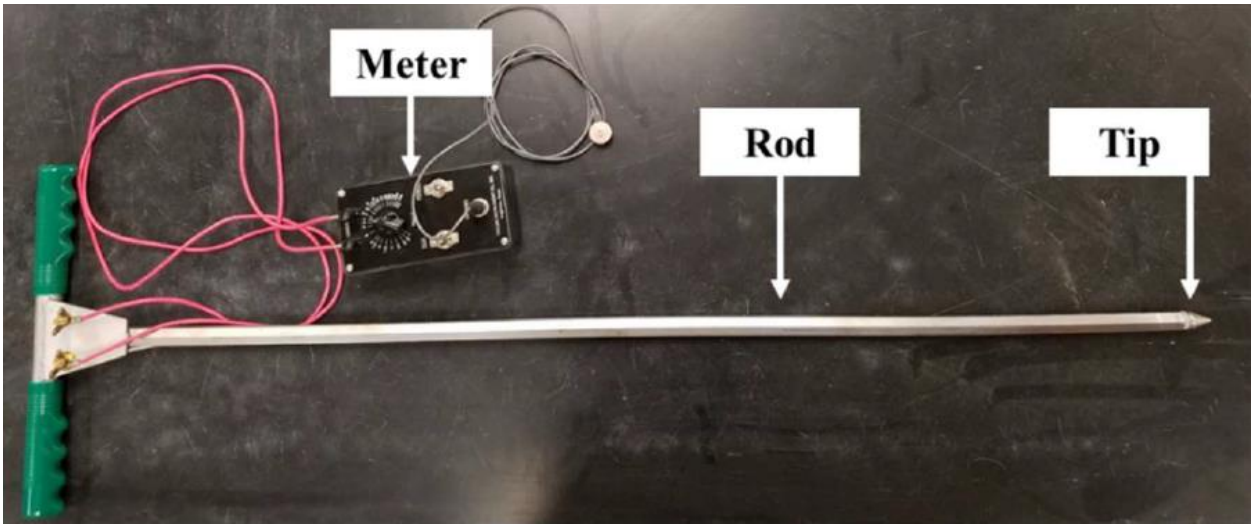

Fig. 2.9 Collins Rod

2.2 MSE Wall Backfill Characterization

KDOT has gradation and electrochemical properties specifications for acceptable aggregate backfill in MSE walls with steel reinforcing strips (Hansen 2015). The electrochemical specifications can be found in Table 2.3. If the resistivity is less than 5,000 Ohm-cm but greater than 3,000 Ohm-cm additional gradation specifications must be met. These

specifications can be found in Table 2.4. Note that the goal of the gradation specifications in Table 2.4 is to limit the percentage of fine grained materials (i.e., material passing the No. 200 sieve) to reduce the likelihood of retaining pore fluid in the backfill, which would further support a corrosive environment. While there are a significant number of specifications that must be met for quality assurance of backfill, these specifications are not measured during the service life to assess the corrosion potential of backfill.

Table 2.3 KDOT MSE wall electrochemical specifications (Hansen, 2015)

Electrochemical Properties	
Measurement	**Requirement**
Resistivity	> 5,000 Ohm-cm
pH	5.0 – 10.0
Organic Content	< 1%
Chlorides Concentration	< 100 ppm
Sulfates Concentration	< 200 ppm

Table 2.4 KDOT MSE wall gradation specifications (Hansen, 2015)

Gradation	
Sieve	**Percent Retained**
100 mm (4”)	0
0.420 mm (No. 40)	40 – 100
0.074 mm (No. 200)	95 - 100

In Kansas, backfill resistivity is measured using AASHTO T 288-12 to determine the corrosion potential. It is a laboratory test that takes a representative soil sample from the field and pulverizes it until the aggregates pass through a 2 mm sieve. Approximately 1,500 g of soil passing the 2 mm sieve are collected and mixed with 150 mL of distilled water and cured for 12 hours. After curing, the sample is remixed and compacted into a soil box of a standard size. The

resistance is measured between the two electrodes on opposite sides of the soil box. The resistivity is calculated using

$$\rho = R * \frac{A}{D} \tag{2.12}$$

where R is the resistance in Ohms, A is the surface area of on electrode in cm^2, and D is the distance between the two electrodes (AASHTO, 2012). The disadvantage of using this method is that it does not exactly mirror the *in situ* conditions.

Another commonly used method to measure soil resistivity and predict the corrosion potential of backfill is ASTM G 57-06 (2012a). Like AASTHO T 288-12, this method utilizes a soil box. Unlike AASHTO T 288-12, this method incorporates four electrodes: a pair of current electrodes and a pair of voltage electrodes. The configuration of this method is shown in Fig. 2.10 with the current electrodes labeled C1 and C2 and the voltage electrodes labeled P1 and P2.

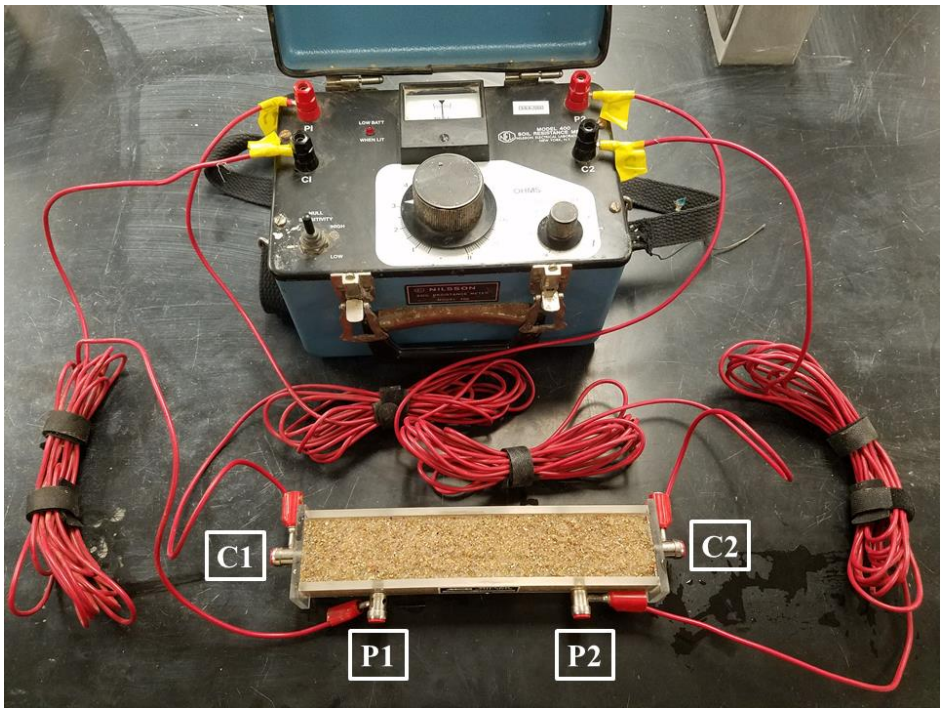

Fig. 2.10 ASTM G 57-06 soil box configuration

A representative soil sample is collected and saturated with distilled water and allowed to reach equilibrium for 24 hours. The sample is saturated to reduce the effects of variations in compaction and moisture content. After sample preparation, the soil mixture is compacted into the soil box. Current is sent through the current electrodes and the resistance is measured in Ohms. The electrical resistivity of the soil sample is calculated using Equation 2.5 where *L* is the distance in cm between the two voltage electrodes (ASTM G57-06, 2012). A temperature correction for the measured resistance should be made when the sample temperature exceeds 21°C using Equation 2.13,

$$R_c = R_T(\frac{24.5 + T}{40}) \tag{2.13}$$

where R_c is the corrected measured resistance in Ohms, R_T is the measured resistance in Ohms, and *T* is the temperature of the soil sample in Celsius. The disadvantage of this method comes with the need to test larger aggregates. Larger aggregates cannot be easily packed into a small space, like a soil box, and ASTM G 57-06 does not set guidelines for how to handle large aggregates. This can lead to inaccurate measurements.

A disadvantage for both AASHTO T 288-12 and ASTM G 57-06 are that they are not *in situ* measurements. *In situ* conditions can be difficult to imitate during sample preparation, and minor changes can lead to large changes in resistivity measurements. Changes due to salinity are explored in Section 3.1.3 of this thesis. In MSE walls, both of these methods are also used only for construction quality assurance and are not used to monitor the backfill environment during the service life of the MSE wall.

The most common way MSE wall backfill is monitored is through the retrieval of buried coupons (Elias et al., 2009). In MSE walls, a buried coupon is a piece metallic wire or strip with no structural benefit. Coupons are placed in groups next to the MSE wall reinforcement at the

face of the wall or end of the reinforcement during construction of the wall. The number of coupons placed requires a monitoring program because the number of coupons dictate how many observations can be made over the service life of a MSE wall. Coupons are later excavated or extracted through the wall face and are weighed and measured. The weight loss and thickness are compared to the original or previous analysis in order to determine the amount of corrosion that has taken place. The disadvantages of a monitoring program that involves metallic coupons are that the coupon's deterioration is not often representative of the all of the MSE wall reinforcement because soil conditions are not completely homogeneous, the method is destructive for the wall, and there are a limited number of tests that can be conducted (Elias et al., 2009).

2.3 Studies on the Corrosion of MSE Wall Reinforcement

A study commissioned by the Utah Department of Transportation assessed metallic MSE wall reinforcement through the extraction of buried metal coupons that were placed during installation (Gerber & Billings, 2010). The objective of the study was to document the extent of corrosion and establish a baseline for which future extraction of coupons could be compared. Twenty-two coupons, all 11-12 years old, were extracted. The study found that the only measurable difference in levels of corrosion were in areas of the coupon that appeared to have been damaged during installation. In other words, where the galvanization was damaged, the coupon displayed more corrosion. All coupons retrieved were within 1.2 m from the wall panel-backfill interface. There was no measurable difference in the level of corrosion between the coupons retrieved based on distance of the coupon from the wall face. No deterioration rate was able to be reliably created because the initial conditions are unknown, but this does lay

groundwork for a future study to measure the deterioration rate of metallic elements in these MSE walls.

Another study in the state of Nevada examined two walls at the intersection of Interstate 515 and Flamingo Rd that had high levels of observed corrosion. The extent of the corrosion was accidentally discovered during construction on top of one wall and during demolition of a section of the other wall. Samples of the backfill were taken to assess its corrosive potential (Thornley & Siddharthan, 2010). It was found that Nevada test T235B, used to measure the resistivity of the backfill, was an inaccurate predictor of soil resistivity and had mistakenly allowed highly corrosive backfill to be implemented in numerous walls in Nevada. In addition to the collection of backfill, an excavation was made in order to see the reinforcement in place. It was found that the reinforcement was uniformly corroding from a distance of 0.6 – 1.5 m away from the wall of the face. These distances were the limits of the excavation. The results of this study concluded that if the walls were left without remediation, they would fail before the 75 year design life.

These two case histories highlight some of the unknowns of existing MSE walls. It is difficult to study MSE walls and give an accurate prediction of service life because conditions behind the wall are not routinely analyzed and recorded in a way that can be used for comparison in future analysis. Establishing baseline measurements and routinely examining MSE walls would be beneficial in more accurately predicting service life and result in fewer surprises.

2.4 Studies on Service Life of Corrugated Metal Pipe

A study in the state of Ohio examined the current conditions of concrete and metal culverts. The objective was to improve the process of estimating the remaining service life of CMP using a multivariable regression model that incorporated the existing CMP corrosion rating

system and other recorded characteristics used by the Ohio Department of Transportation (ODOT) (Urrea, 2014). The existing corrosion rating system was on a scale of 0 – 9 with zero being CMP failure and 9 being new and undamaged. Some of the characteristics recorded and used in the model were slope, length, age, thickness, surrounding soil type, pH, and the corrosion rating. Many of these characteristics have been recorded and used in other studies (Stratton, 1990). Twenty one metal CMP were analyzed. A linear model was created with the collected data that had a coefficient of determination of 0.874. Although this research was limited in the number of pipes analyzed, this model could be used as the foundation for predicting the service life in Ohio and act as a framework for a larger study in Ohio. Refining the model could result in a more accurate prediction of service life of CMP than the current standard for estimation, California test 643, predicts. The model could be adapted for different DOTs and their differing corrosion rating systems. For example, KDOT's rating system has been based on a scale of 1 – 100 instead of 0 – 9 like Ohio (Stratton, 1990).

Two studies were conducted by the KDOT Bureau of Materials and Research investigating the performance of CMP in Kansas. The first study, conducted in 1989, was aimed at evaluating the corrosion of CMP installed with a lighter gauge than the CMP used previously (Stratton, 1989). It encompassed approximately 100 CMP installed between 1977 and 1989. The analyzed CMP were chosen because they were a part of ten different projects located in ten different counties across the six KDOT districts. The counties where the projects were located are highlighted in Fig. 2.11.

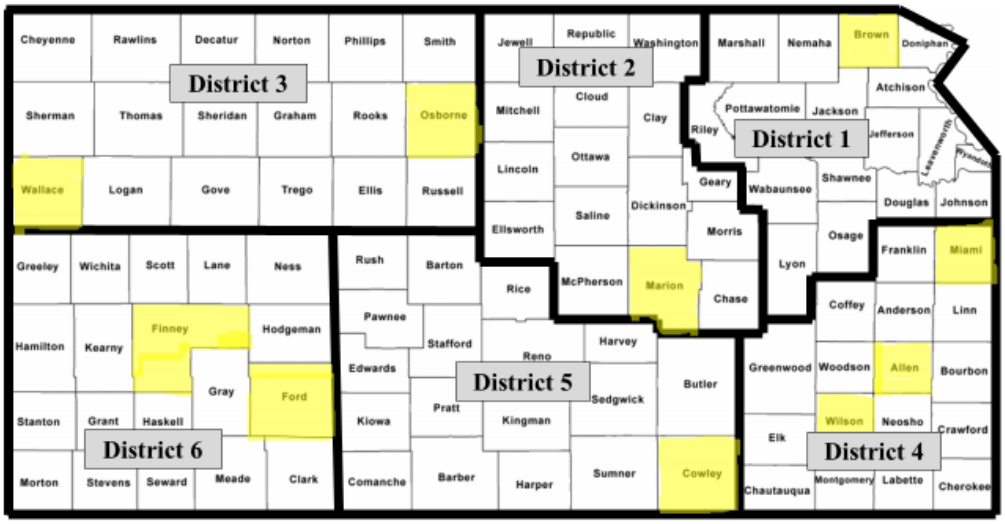

Fig. 2.11 Location of CMP involved in the 1989 study in the State of Kansas

Each CMP examined filled a data set that included the galvanization thickness, CMP thickness and diameter, photos of the CMP without any cleaning or alteration, and a corrosion rating that characterized the current state of the entire CMP. The rating system used was on a scale of 1-5 and can be found in Table 2.5.

Table 2.5 1989 Corrosion Rating System (Stratton, 1989)

Rating	Description
1	Pipe in excellent condition
1+	Pipe in excellent condition. Minor inlet or outlet damage or erosion. Light silt and/or oxidation
2	Pipe in good shape. Heavy oxide film. 0-40% silting and/or minor to moderate inlet or outlet damage.
2+	Pipe in reasonable good shape. Heavy oxide film. May have 40-50% silting. May have moderate to heavy inlet &/or outlet damage. Minor settling or distortion.
3	Pipe Rusting. No distortion or settling. May have silting.
3+	Pipe rusting. Distortion &/or settling. May have silting.
4	Pipe heavily rusted with distortion and/or settling. May have silting.
5	Pipe failed. Because of distortion, collapse, rusting, or complete silting.

The study found, based on age and corrosion rating, that within the following ten to fifteen years, over 50% of the CMP examined would be perforated by rust or collapse completely. Stratton (1989) concluded that possible causes of the rapid deterioration, mostly found in the eastern part of the state, were the suspicion of highly acidic drainage resulting from agricultural runoff, and heavy silting paired with poor drainage. The agricultural runoff removed the galvanization faster than typical rainwater while the silting would have created an environment more prone to corrosion because of the capacity to trap moisture. Stratton (1989) recommended increased care during installation and development of a maintenance program in order to slow the corrosion and extend the service life of the CMP.

The second study was a follow-up that inspected 819 CMP from a wider range of ages throughout all six KDOT districts across 40 separate projects. This study was prompted by conflicting reports of CMP deterioration in Kansas (Stratton, 1990). The objective was to investigate the findings of Stratton (1989) and identify why CMP installed within the last 13 years were deteriorating much faster than those installed at an earlier date. For this study, an updated rating system found in Table 2.6 was used. Using this rating system it was confirmed that CMP installed after 1975 were deteriorating at a faster rate than those installed before 1975. After an investigation into the material used for the CMP, it was found that KDOT's design recommendations for CMP changed. The new recommendations allowed for a lighter gauge (thinner) CMP. It was this reduction in thickness, both to the steel and the galvanization, which most likely influenced the decline in expected service life of CMP installed after 1975.

Table 2.6 1990 Corrosion Rating System (Stratton et al., 1990)

Rating	Description
95-90	Spelter like new to very dull
87.5	Pinpoint rust
85	Spelter entirely gone
80	Light rust film
70	Shallow pitting
60	Scaley rust or pits not ½ through metal
45	Heavy rust or pits ½ through metal
30	Heavy rust or pits ¾ through metal
15	Few holes through metal
0	Large areas of metal gone

Stratton (1990) concluded that most CMP in the study had 25 or more years of service life left based on the remaining thickness of the CMP. However, the prediction was site specific and dependent mostly on accurate pH and resistivity measurements taken in accordance with California test 643. Stratton (1990) concluded most CMP in the study from the previous 50 years had performed well, but the site characteristics (pH and resistivity) and material properties (gauge) needed to be carefully considered when attempting to accurately predict the service life.

2.5 Summary

This literature review establishes the common types of corrosion observed in CMP and links the severity of that corrosion to the rating system used by Stratton (1990) and for this research. Additionally, factors affecting corrosion, including electrical resistivity and salinity, were discussed because these were investigated further in conjunction with CMP deterioration and MSE wall backfill conditions. Electrical resistivity was discussed in depth to understand the

selection of array types used and outline the influence of characteristics like pore-water saturation and salinity, both of which were investigated further as part of this research.

Chapter 3 - Methodology

3.1 Experimental Methodology for Corrugated Metal Pipe

The experimental methodology for assessing CMP included the creation of an ArcGIS database and recording the field observations within that database. Laboratory testing for the CMP included ion chromatography and a soil box resistivity experiment.

3.1.1 ArcGIS Database and Field Observations

The CMP examined in this study were located and identified using construction plans found in the KDOT project database ProjectWise. To store the location and data set for each CMP, a map, shown in Fig. 3.1, was created using ArcGIS Online and the ArcMap desktop application. The location of each CMP is displayed as a node on the map. Because of the closeness of some CMP to one another, not all nodes are visible due to overlap.

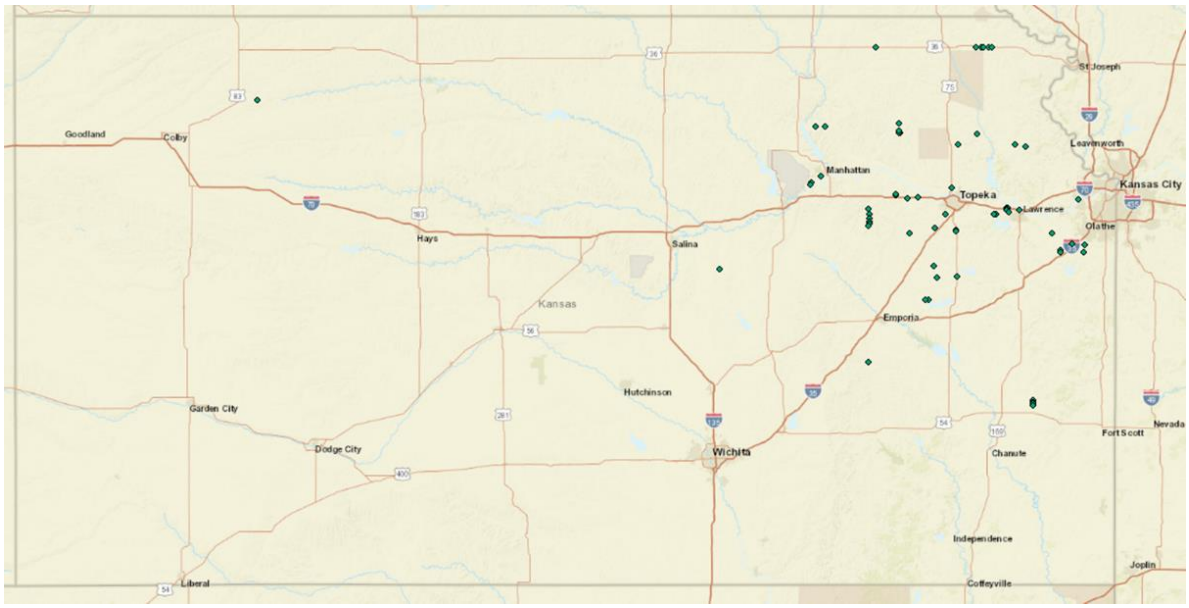

Fig. 3.1 Location of CMP involved in the 2018 study in the state of Kansas

The dataset for each CMP contains dimensions (e.g., diameter, pitch, and depth), identifiers (e.g., project number, county, material, and age), *in situ* measurements (e.g., resistivity

and corrosion ratings for the invert, side, crown, and external faces), and accompanying photos and description. The corrosion ratings for the four faces were measured using a system similar to the one created by Stratton et al. (1990). The rating system used for this study, found in Table 3.1, does not include a rating of 100 because that rating was reserved for CMP installed within one year of the study being conducted for which there were no CMP that fit that criteria.

Table 3.1 Corrosion rating system

Rating	Description
95	Spelter like new
92	Spelter dull
90	Spelter very dull
88	Pin-point rust spots
85	Spelter entirely gone
80	Light rust film
70	Shallow pitting
60	Scaley rust or pits not ½ through metal
45	Heavy rust or pits ½ through metal
30	Heavy rust or pits ¾ through metal
15	Few holes through metal
0	Large areas of metal gone

The visible corrosion of most CMPs analyzed in this study was not uniform over the entire surface. In order to more accurately record the observed corrosion, each end of all of the CMP were divided into four different faces. The divided faces, found in Fig. 3.2, were labeled crown, side, invert, and external. The interior of the CMPs had more divisions than the exterior because the interior exhibited more varied levels of corrosion throughout. In addition to the division of the ends, each end of all CMPs were rated because some pipes exhibited different levels of corrosion at each end. Each end was assigned the letter *A* or *B*, based on the relative

direction in which it laid; ends designated *A* were the northernmost or easternmost of the two ends and ends designated *B* were the southernmost or westernmost.

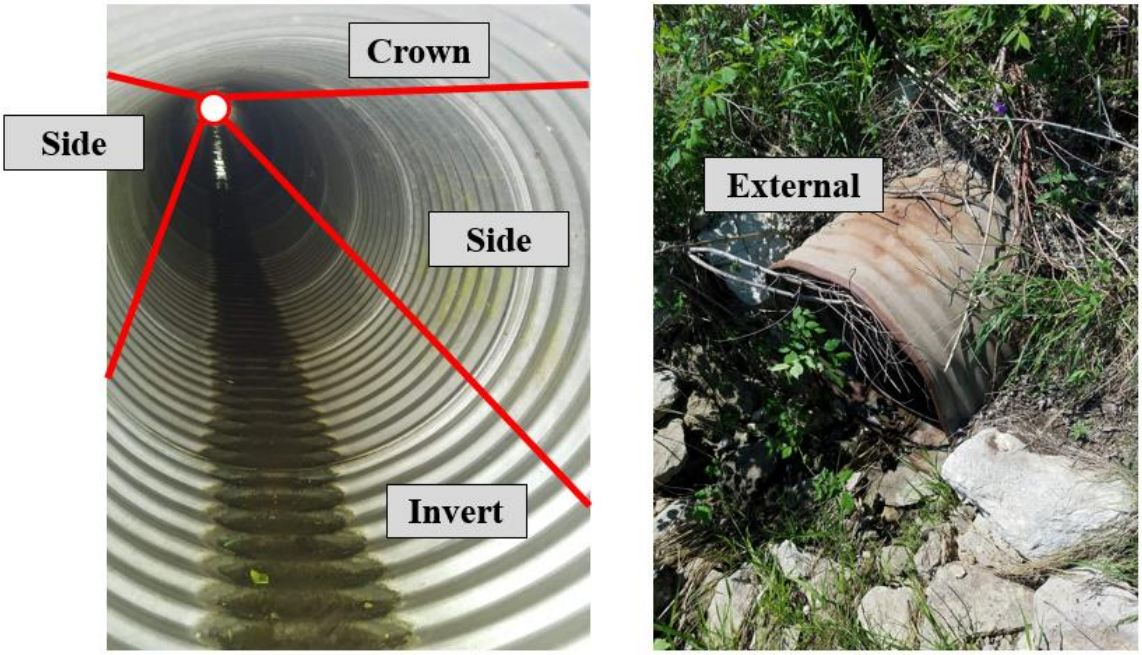

Fig. 3.2 Corrugated metal pipe faces

In addition to recording the observed corrosion, the resistivity of the soil surrounding each CMP was measured using a Collin's rod apparatus. To measure the resistivity of the soil, the rod was driven approximately 0.3 m into the ground. Three separate measurements were taken at the end of the CMP with the lowest general condition rating. All three measurements were taken down by the invert and within 1 m of the CMP and were averaged to get one general resistivity measurement for the soil surrounding the pipe.

3.1.2 Soil Box Resistivity

Due to high variability of in situ resistivity (see Results, Fig. 4.6), the effects of salinity due to roadside deicers on resistivity were measured with a laboratory electrical resistivity test. The soil used was a poorly graded sand mixed in the laboratory and classified using the Unified Soil Classification System (ASTM D2487-17, 2017). The sand was divided into several samples

and each sample was fully saturated with deionized water mixed with salt. Several different dissolved salt concentrations were tested with each concentration being measured twice. The concentrations were chosen based on the findings of Li et al. (2015) to represent salinity from road deicers. The electrical resistivity was determined in accordance with ASTM G 57-06 (2012a) using a Nilsson Resistance Meter Model 400 attached to a M.C. Miller Large Soil Box. The apparatus can be seen in Fig. 2.10 with the current electrodes labeled as C1 and C2 and the voltage electrodes labeled as P1 and P2.

The results from the soil box test can be found in Table 3.2. They confirm common knowledge: soil resistivity decreases as ion concentrations increase (Everett, 2013). In this case, the ions were dissolved salts. This experiment shows that even a minor presence of dissolved salts can drastically change the resistivity of a soil. It also introduces a concern about resistivity as a means to predict corrosion of CMP. Dissolved salts are more prevalent in winter months because of the application of road deicers (Herb, 2017). This increase in dissolved salts, and subsequent lower soil resistivity, could lead to an overconservative estimation of service life of a CMP. Conversely, resistivity measured in the summer with the absence of road deicers and a higher soil resistivity could lead to an overprediction of the service life of a CMP. In addition to the field measured resistivity this preliminary analysis supported the additional ion chromatography measurement.

Table 3.2 Results from soil box resistivity testing

	Trial 1 (0 ppm)	Trial 2 (0 ppm)	Trial 3 (100 ppm)	Trial 4 (100 ppm)	Trial 5 (1,000 ppm)	Trial 6 (1,000 ppm)	Trial 7 (2,500 ppm)	Trial 8 (2,500 ppm)
Resistance (Ohms)	11,000	11,500	9,500	10,500	2,650	2,600	1,400	1,550
Corrected Resistance (Ohms)	12,237	12,794	10,569	11,681	2,948	2,893	1,558	1,724
Resistivity (Ohm-m)	97.9	102.4	84.6	93.5	23.6	23.1	12.5	13.8

3.1.3 Ion Chromatography

Soils surrounding selected CMP were tested to measure the chloride concentration contained in the soil. This was done as an investigation into alternative soil properties to resistivity that could be used to predict corrosion. Not all CMP were chosen for analysis. CMP were chosen based on age and deterioration rate. The deterioration rate, calculated for the invert of CMP, was found using Equation 3.1,

$$D = \frac{95 - I}{A} \tag{3.1}$$

where D is the deterioration rate of the CMP, I is the invert rating based on the corrosion rating system found in Table 3.1, and A is the age of the CMP. The invert rating was chosen because it had the most variability in ratings. This variability will be discussed more in Chapter 4. The value of 95 was used because that was the highest rating any CMP in the study received. A rating of 100 was reserved for CMP installed the same year as the inspection. There were no CMP that met this criteria. The pipes were selected in order to represent the range of ages and deterioration rates found within the age groups. The chloride concentrations were measured by

the Kansas State University Research and Extension Soil Testing Lab (Soil Testing Lab). To separate the soil and water, a leachate test was conducted. The leachate test conducted was similar to the USGS Field Leach Test (Hageman, 2007). In the USGS test, 50 g of soil was collected and placed in a graduated cylinder where 1 L of deionized water was added. In order to not fully saturate the deionized water with the ions contained in the soil, 50 g of soil was chosen. This mixture was shaken for five minutes and allowed to settle for ten minutes. The mixture was dispensed into beakers where pH and other characteristics could be easily measured and the mixture could be filtered as desired. In contrast to the USGS test, for this research, 100 g of soil was collected and mixed with 1 L of deionized water in an Erlenmeyer flask. A larger amount of soil was collected because the ion concentrations within the soils were expected to be low, therefore ion saturation of the deionized water was not a concern. Additionally, more soil was collected in order to have a high enough ion concentration to be detected by the IC system used by the Soil Testing Lab. After shaking and settlement, the mixture was centrifuged at 12,100 rpm for ten minutes in order to separate the soil from the water. The separated water was stored in a refrigerator until processed. Any additional filtration was conducted by the Soil Testing Lab. Deviating from the USGS test, the soil was placed back into the Erlenmeyer flask and 1 L of new deionized water was added. This was done in an attempt to mobilize remaining chlorides contained in the sample. The mixture was shaken and let settle for 24 hours. The mixture was separated and stored in the same manner as before. These steps were done three times in order to collect three water samples in addition to the initial water sample.

3.2 Experimental Methodology for Mechanically Stabilized Earth Walls

The experimental methodology for assessing MSE walls included determining the appropriate locations for resistivity surveys at the top and bottom of the walls. Various other

tests were conducted to develop the experimental methodology and to better understand the effects of certain elements in the experiment, including penetration depth of stakes, time intervals between tests, and measurement time. It was important to explore these elements because of the unique and uncommon nature of the experiment, specifically the length of the stakes and the manner in which electrical resistivity was used.

3.2.1 Methodology Development

Three series of resistivity tests were conducted to better understand the equipment, primarily the extra-long stainless steel stakes, for the unique application of electrical resistivity used in the into-the-wall surveys. The stainless steel stakes, 90 cm long, were specifically fabricated for the into-the-wall resistivity surveys. These stakes are approximately twice as long as a standard stake. Both stakes can be found in Fig. 3.3.

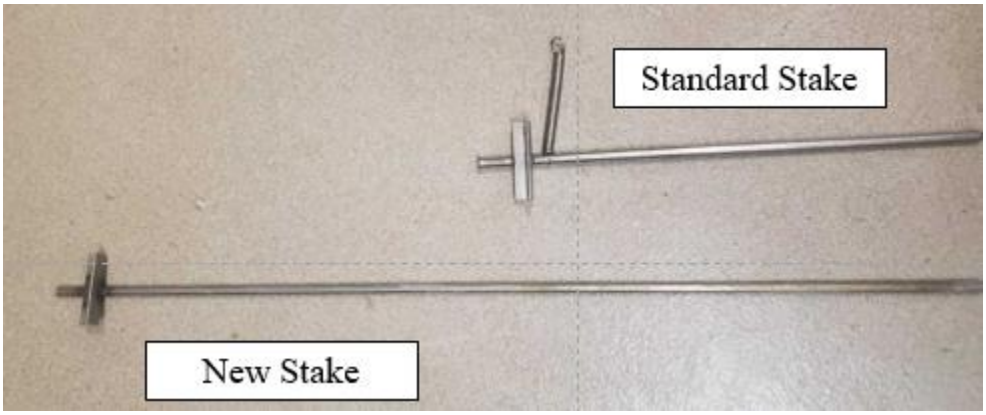

Fig. 3.3 Standard and new stake

The first test was to examine the effects of charge buildup on these stainless steel stakes as a result of running multiple arrays in succession. The concern was that the stakes would not fully discharge the charge gained from sending a current through the stakes to the backfill because a large portion of the stake was not in contact with soil as it had to by-pass the thick (i.e., 30 cm) MSE wall panel. Six different arrays were tested in the same order at two different

time intervals. The first time interval was set at one minute between the end of one array and the start of another, the second time interval was set at five minutes. The results from both time intervals were nearly identical, indicating that charge buildup on the stakes did not influence the resistivity reading of each successive array; the results are located in Table 3.3. The time interval chosen for the research done for this thesis was approximately one minute.

Table 3.3 Results of interval tests

1 Minute Interval		**5 Minute Interval**	
Array	**Resistivity (Ohm-m)**	**Array**	**Resistivity (Ohm-m)**
Dipole-Dipole	35.1	Dipole-Dipole	35.4
Wenner	32.5	Wenner	32.5
Schlumberger	32.4	Schlumberger	32.4
Inverted Schlumberger	32.6	Inverted Schlumberger	32.5
Merged: Dipole-Dipole / Wenner	33.7 – 34.4	Merged: Dipole-Dipole / Wenner	33.6 – 34.4
Merged: Dipole-Dipole / Schlumberger	33.7 – 34.5	Merged: Dipole-Dipole / Schlumberger	33.6 – 34.4

The second test was conducted to observe the changes in resistivity measurements based on the penetration depth of the stainless steel stakes used for the into-the-wall surveys. The panels of the MSE walls in this study varied in thickness, causing a variation in the depth at which the stakes could be driven into the backfill perpendicular to the wall panels. Therefore it was important to understand the variance in resistivity measurements based on a range of penetration depths likely encountered in the field. The concern was that current would be lost to the air as it traveled down the extra length of the stake. Inadequate current into the ground often results in negative resistivity measurements (AGI, 2009). Negative measurements are not physically possible, indicating error in the measurement.

To test the effects of penetration depth, the four, 90 cm long stakes used for measurements into the face of the MSE walls were driven into the ground, in a straight line, with a 0.5 m spacing between each stake. Each stake was first driven to a depth of 20 cm from the surface of the ground to the embedded tip of the stake. This was followed by using a dipole-dipole array to measure the resistivity at that depth. After the array was run, each stake was driven an additional 10 cm into the ground and, again, the dipole-dipole array was run. This process occurred a total of four times, with the final penetration depth being 50 cm. The results from this test are located in Table 3.4. This test showed that penetration does have an impact on the resistivity measurement. While the resistivity may have varied because of the heterogeneity of the soil, it is more likely that the resistivity was lower as penetration depth increased due to the better contact with the ground and less current lost to the air. Note in Table 3.4 that as the depth of penetration increased the resistivity degreased, almost linearly. Also the site where this experiment was conducted has a relatively heterogeneous soil layer near the surface. For this research, a penetration depth of 30 cm was used. Given the thicknesses of the wall panels, it was not possible to achieve a penetration depth into the backfill much deeper than 30 cm because the seat at which the electrode is fastened to the stake would come in contact with the wall face. If the stake and wall face touched, current would be diverted from the backfill to the wall face resulting in inaccurate data. Note that although the stake penetration did influence magnitude of the measured resistivity, the differences were not significant considering the range of resistivity anticipated in corrosive MSE walls. In other words, a dry sandy material would have a measured resistivity of approximately 200 Ohm-m while a saturated sand with corroded steel would have a measured resistivity of 20 Ohm-m. Thus the changes shown in Table 3.4 were negligible for the purposes of this research.

Table 3.4 Results of penetration depth test

Penetration Depth cm (inches)	Resistivity (Ohm-m)
20 (7.87)	39.3
30 (11.81)	35
40 (15.75)	31.2
50 (19.69)	27.7

The third test of the resistivity equipment was conducted at an MSE wall to observe the change in resistivity based on measurement time. This is the amount of time current is injected into the backfill. The standard measurement time used most commonly was 1.2 seconds. However, some backfills did not produce electrical resistivity measurements at the standard measurement time. The backfills in which this problem manifested had poorer contact resistance, likely from larger gravel aggregates. In an effort to solve this problem, the measurement time was increased up to a duration of 14.4 seconds. The results, found in Table 3.5, show a slight increase in the resistivity measured as the measurement time increased for both of the array types tested. This increase in resistivity is negligible. A reading was not recorded for the Wenner array at a measurement time of 14.4 seconds because of an error with the file. For the main study, a measurement time of 1.2 seconds was used when possible. Longer durations were used only when necessary to obtain a resistivity measurement.

Table 3.5 Results of measurement time testing

Array	Measurement Time (s)	Resistivity (Ohm-m)
Dipole-Dipole	1.2	67.3
Dipole-Dipole	3.6	68.6
Dipole-Dipole	7.2	69.5
Dipole-Dipole	14.4	69.7
Wenner	1.2	47.5
Wenner	3.6	48.1
Wenner	7.2	49.2
Wenner	14.4	---

3.2.2 Location of Surveys

The SuperSting Earth Resistivity, IP & SP System (SuperSting), created by Advanced Geosciences, Inc. (AGI), was used to measure and collect the electrical resistivity data for each MSE wall. Each MSE wall was surveyed at both the top and bottom.

Fig. 3.4 shows a typical MSE wall cross section and the location of the two surveys noted as A and B.

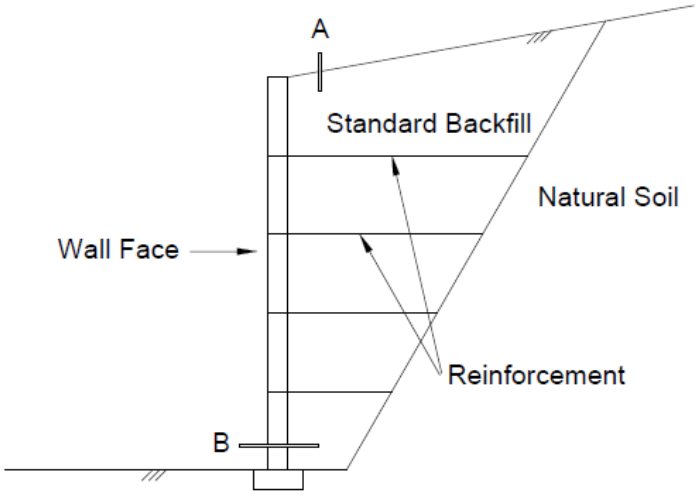

Fig. 3.4 Location of resistivity surveys at an MSE wall

The survey at the bottom of the wall (point B in Fig. 3.4) began with the drilling of four evenly spaced holes, parallel and equidistant from the ground, because the survey needed access to the backfill at the base of the wall. These holes were drilled carefully, to only go through the wall panels and avoid the reinforcement strips. The holes were drilled so the concealed backfill was minimally disturbed and to ensure that the holes were drilled as close to perpendicular to the wall face as possible so the electrodes could be installed. After the holes were drilled, four 90 cm long stakes were driven 30 cm into the backfill through the holes. These stakes were stabilized by wood shims in order to avoid contact with the wall panel. Contact with the wall panel would direct current running through the stake away from the backfill and into the wall panel, resulting in inaccurate resistivity measurements. The completed installation of a stake can be seen in

Fig. 3.5. The depth of investigation for the electrical resistivity measurements was checked to ensure that the native soil behind the backfill had minimal to no impact on the measurements taken into-the-wall. If the depth of investigation was too deep or too far into the backfill, the electrical resistivity measurements taken would not purely represent the backfill. Depth of investigation was calculated using Equations 2.10 and 2.11.

Fig. 3.5 Electrode and stake setup for into-the-wall electrical resistivity surveys

Following the completion of the survey setup, a contact resistance test was executed. A contact resistance test ensures proper connection between the electrodes and the stainless steel stakes, as well as adequate contact between the stake and the soil. For the backfill, which was granular, adequate contact was around 1,500 Ohms. Stakes were not be redriven to improve the contact resistance because it did not improve the contact resistance and it disturbed the backfill. Having confidence in the outcome of the contact resistance test provides more confidence in the resistivity measurements taken during the actual electrical resistivity surveys. Following a satisfactory contact resistance test, the surveys were run and the files were brought back to the office to be processed. The surveys run included a series of six different four-electrode comprised of four individual arrays: Dipole-Dipole, Wenner, Schlumberger, Inverted Schlumberger, and two merged arrays: Dipole-Dipole/Wenner and Dipole-Dipole/Schlumberger

In addition to the surveys run into-the-wall, a survey at the top of the wall (point A in Fig. 3.4) was conducted at walls where permitted; walls topped with soil allowed for surveys to be run at the top while walls topped with rip-rap or pavement did not due to the lack of good contact between the stakes and soil. To run a survey at the top of the wall, 28 stainless steel stakes were driven approximately 30 cm into the backfill parallel to and within a range of 1 m to 2 m of the wall face. This distance from the wall was chosen because the influence of the wall panel resistivity on the survey is lost at a distance equal to the electrode spacing (Snapp et al., 2017). This loss is important because the air on the opposite side of the concrete wall panels is infinitely resistive which could increase the bulk measurements of the surveys at the top of the wall if they were too close to the wall face. The spacing between stakes were constant for entire surveys, but varied from survey to survey and wall to wall in order to reach a target depth (i.e., the bottom of the walls). Spacing for entire surveys ranged from 0.5 m to 2 m. After the stakes were driven into the ground, the electrodes were attached to the stakes in and the SuperSting

System was attached to the front end of the electrode line. Both the Schlumberger and Dipole-Dipole arrays were run at the top of the wall because of their proficiency in detecting horizontal layers. The objective at the outset of this work was to potentially capture a layer of lower resistivity backfill sandwiched between higher resistivity backfill and very low resistivity natural soil. The effectiveness of the top-of-the-wall surveys will be discussed in Chapter 4. A completed setup can be viewed in Fig. 3.6.

Fig. 3.6 Resistivity survey setup for top-of-the-wall electrical resistivity surveys

3.2.3 Backfill Sample Collection

Samples of the MSE wall backfill were collected at each site. A square hole, approximately 20 cm by 20 cm, was cut using a concrete saw at the base of the wall within the bounds of the into-the-wall resistivity surveys. An example of the backfill collected can be found in Fig. 3.7. The backfill was collected for laboratory testing in an effort to support the into-the-wall resistivity measurements. Testing included moisture content and grain size

distribution. All laboratory testing was conducted by the University of Kansas. Using the moisture content, the degree of saturation, *S*, was calculated using Equation 3.2

$$S = \frac{G * \omega}{e} \tag{3.2}$$

where *G* is the specific gravity, ω is the moisture content, and *e* is the void ratio. The specific gravity was assumed to be 2.65, an approximate value for most cohesionless soils, and the void ratio was roughly estimated using the Unified Soil Classification System (USCS) classification (Holtz et al., 2011).

Fig. 3.7 MSE wall backfill sample collection

3.2.4 Summary

The various tests discussed in Section 3.2.1 helped develop the experimental protocol for the use of electrical resistivity in a unique manner. For the tests conducted at the MSE walls, the interval at which tests were run was roughly one minute, the depth of penetration of the stakes were 30 cm, and the measurement time was 1.2 seconds whenever possible. Changes in the

measurement interval and measurement time were shown to not have a great effect on the measurements collected. The depth of penetration had a pronounced effect on the resistivity measurements. For this reason, the stakes were driven in as far as possible (approximately 30 cm). After the experimental protocol was established, electrical resistivity surveys were run at the MSE walls. Four holes were drilled into the face of the wall in order to take a series of four electrode measurements. Six different four point arrays types were used to measure into-the-wall to assess the corrosion potential of the backfill based on electrical resistivity. A top of the wall survey spanning 28 electrodes was conducted wherever permissible in an attempt to cross validate the into-the-wall measurements.

Chapter 4 - Results and Discussion

4.1 Overview

This chapter includes the results gathered for the CMP and MSE wall study. Only one sample CMP is discussed in detail followed by the overarching observations about all CMP in the study. The complete data sets for each CMP can be found in Appendix A. The results for the MSE wall are sectioned by each individual wall. A comprehensive table regarding the characteristics of the MSE walls can be found in Appendix B.

4.2 Corrugated Metal Pipe

Corrugated metal pipe diameters in the United States are listed in inches. In this text, the diameters will be listed in inches with the accompanying diameter nominal measurement in parenthesis.

4.2.1 Sample Corrugated Metal Pipe

CMP K-63/80yr is located on highway K-63, in Pottawatomie County, North of St. Marys, Kansas. It was 78 years old at the time of the survey and is a galvanized CMP with a diameter of 24 inches (600 mm). Both Side A (Fig. 4.1) and Side B (Fig. 4.2) of CMP K-63/80-yr were inspected. As with all CMP examined in this study, pictures and data were recorded for the four faces previously defined in Fig. 3.2. Some CMPs exhibited the same amount of corrosion on both ends while others, as is the case CMP K-63/78yr, displayed different levels of corrosion on each end. The diameter was confirmed to be 24 inches (600 mm) using a tape measure. The CMP pitch was 2.67 inches (70 mm) and depth was 0.5 inches (13 mm), both measured with a ruler. This diameter, pitch, and depth was a standard CMP profile measured in this study.

Fig. 4.1 Side A of sample CMP K-63/80-yr, (a) external, (b) internal

The external face of Side A displayed light rust film near the soil cover (Fig. 4.1a). Inside of the pipe, both the crown and side faces had lost the entirety of their spelter, while the invert had lost large areas of metal (Fig. 4.1b). These ratings were converted to the numerical values 80 for the external face, 85 for the crown, 85 for the side, and 0 for the invert in order to calculate the average value. This value, labeled general condition, was found to be 62.5 for Side A. The other end of the pipe, Side B, also showed light rust film on the external face (Fig. 4.2a). Its interior faces were also similar in that both the crown and side faces had lost their spelter (Fig. 4.2b). The difference between the two ends were found in the invert, where Side B had not lost any material. The invert of Side B exhibited heavy rust approximately ¾ through the metal; it did appear to be nearing the manifestation of holes because of the heavy rust (Fig. 4.2b). The converted numerical ratings were 80, 85, 85, and 30. The resulting general condition for Side B was found to be 70. Table 4.1 shows a complete dataset for the sample CMP. A Collins rod soil resistivity rod was used in three separate locations near the CMP to determine the average resistivity of the soil surrounding the CMP to be 700 Ohm-cm.

Fig. 4.2 Side B of sample CMP K-63/80-yr, (a) external, (b) internal

Table 4.1 Collected data of sample CMP K-63/80-yr

Data Field	User Input	Data Field	User Input
Project Number	K-63	General Condition (A)	62.5
County	Pottawatomie	External (A)	80
Material	Galvanized	Crown (A)	85
Age (yr)	80	Side (A)	85
Diameter / in (mm)	24 (600)	Invert (A)	0
Pitch / in (mm)	2.67 (70)	General Condition (B)	70
Depth / in (mm)	0.5 (13)	External (B)	80
Resistivity (Ohm-cm)	700	Crown (B)	85
Description	Not Applicable	Side (B)	85
Photos	Shown Right	Invert (B)	30

4.2.2 Observed Ratings of Corrugated Metal Pipe

The CMP corrosion ratings for each face were divided into age groups for analysis, shown in Fig. 4.3. The age groups were selected to match those used by Stratton et al. (1990). Only one end of each pipe was included in the analysis. The end exhibiting the most overall corrosion (i.e., lowest general condition rating) was selected as a representation of the worst case scenario for each CMP. In Fig. 4.3, the dotted line between the 35-44 and 45-54 year old groups represents the policy change KDOT implemented in 1975 allowing for lighter gauge (thinner)

CMP to be used. The solid line between the 15-24 and 35-44 year old groups represents the reversal of the 1975 policy change to pre-1975 gauge requirements.

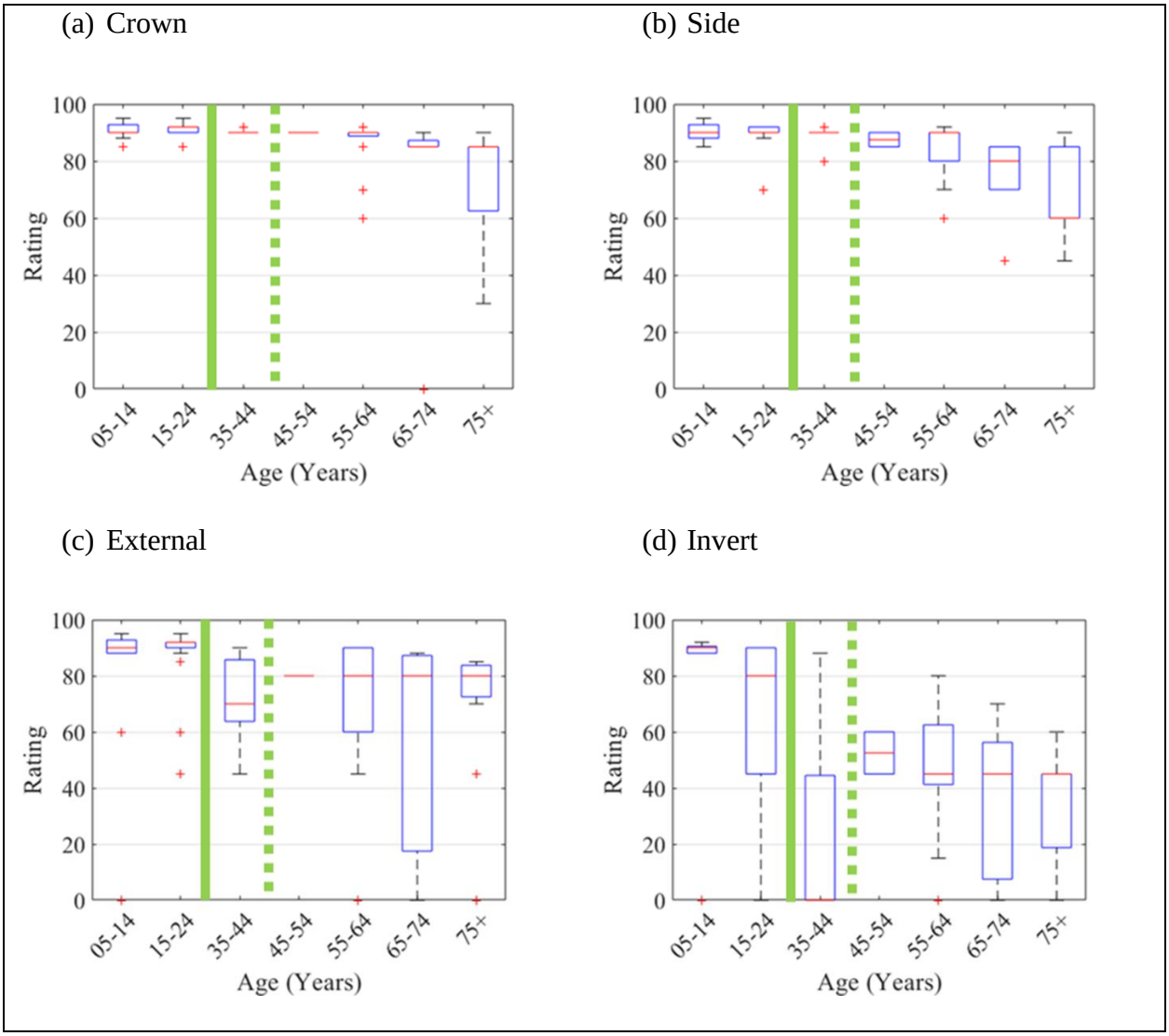

Fig. 4.3 Corrosion ratings grouped by age, (a) external, (b) crown, (c) side, (d) invert

The crown of the observed CMP showed a decline in the corrosion as age increased (Fig. 4.3a). This was an expected decline as material will degrade over time after installation. The side of the CMP also showed a similar decline in rating as age increased (Fig. 4.3b). The external face of the CMP had a much higher variance in rating (Fig. 4.3c). However, this variance does not necessarily indicate that corrosion was the only factor. Many of the CMP observed had

crumpled exteriors, likely a result of impact from a tractor or other vehicle. The crumpled exteriors created surfaces for water to be caught on, artificially accelerating the rate of corrosion on the exterior of the CMP.

The CMP face with the highest variability was the invert (Fig. 4.3d). This variability was attributed to differing levels of corrosion. Many of the inverts contained sediment, fostering a setting that increases the rate of corrosion due to the deprivation of oxygen and increased contact with moisture. The covered areas of the CMP became more anodic relative to the uncovered areas of the CMP, creating an electrode potential imbalance and leading to accelerated corrosion (Cicek 2014).

The invert was determined to be the most valuable component when analyzing the corrosion of CMP due to its high variability and non-linear changes across age groups. Therefore, CMP characteristics believed to further contribute to corrosion were selected to measure against the invert ratings. The first characteristic chosen was the corrugation depth because of the capacity for deeper corrugations to trap more sediment in the invert. Only two corrugation depths, 0.5 inches (13 mm) and 1 inch (25 mm), were measured in this study. The 1 inch (25 mm) corrugation depth was only found in two age groups, 35-44 and 75+ years old (Fig. 4.4), and was far less common than the 0.5 inch (13 mm) corrugation depth; only 1 out of 80 had a depth of 1 inch (25 mm). In Fig. 4.4a, the average invert rating for 1 inch (25 mm) depth is zero because each CMP invert in this age group with a depth of 1 inch (25 mm) was rated zero. Fig. 4.4 results are inconclusive because one depth dimension does not have higher invert ratings in both age groups.

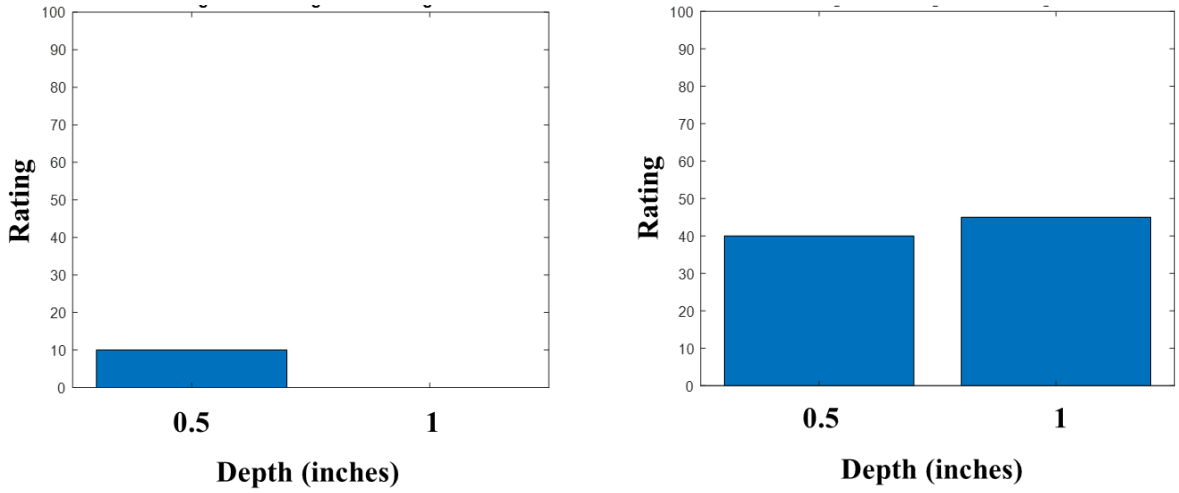

(a) Age 35 – 44 Average Invert Rating (b) Age 75+ Average Invert Rating

Fig. 4.4 Average invert rating with corrugation depth (a) age 35-44, (b) age 75+

The second characteristic chosen to measure against invert rating was the CMP material (Fig. 4.5). Only two age groups were analyzed because only the 5-14 and 15-24 year old age groups had materials alternative to galvanized CMP. This is a result of KDOT's policy for not allowing anything but galvanized CMP prior to 2001 (Stratton et al 1990). The three material types analyzed were galvanized, aluminized, and aluminum. In Fig. 4.5b, no aluminized CMP were observed. From Fig. 4.5, it can be seen that while one material does not rate the highest in both age groups, traditional galvanized CMP is not the highest rated CMP in either age group.

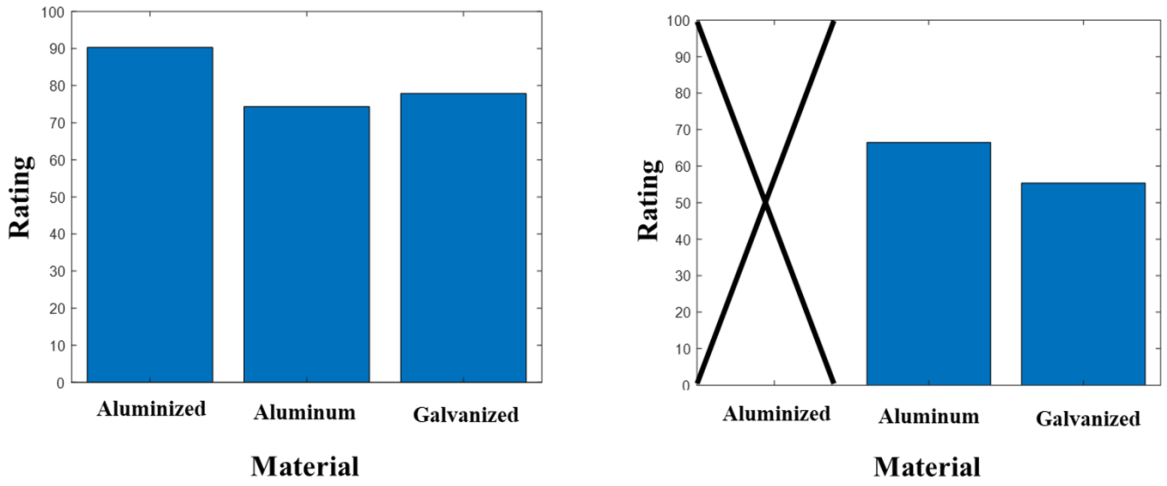

(a) Age 05 – 14 Average Invert Rating (b) Age 15 – 24 Average Invert Rating

Fig. 4.5 Average invert rating with material type (a) age 05-14, (b) age 15-24

To further investigate performance of CMP relative to one another, the average deterioration rates were calculated for groups of CMP based on KDOT policy changes affecting gauge thickness and material type. Found in

Table 4.2, the time periods chosen were pre-1975, 1975-1989, and 1990 or 2001 – Present. These time periods represent initial KDOT standards, the standards allowing lighter gauged CMP, and a return to the original standard gauge requirements, respectively. The aluminum and aluminized pipe material groups start in 2001 instead of 1990 because these materials were not allowed by KDOT until 2001. These data show a higher rate of deterioration of galvanized CMP installed between 1975 – 1989 than any other group, indicating a faster degradation of the CMP installed during that era and shorter expected service life.

Table 4.2 Deterioration rate of inverts

Time Period	Materials	Average Rate of Deterioration
Before 1975	Galvanized	0.79
1975 – 1989	Galvanized	1.84
1990 – Present	Galvanized	1.17
2001 – Present	Aluminized	1.00
2001 – Present	Aluminum	1.32

Two properties of the soil surrounding the CMP were investigated in an attempt to find an indicator of expected deterioration rate. Electrical resistivity was first chosen because it is accepted as an indicator of corrosive environments and is used in California Test 643 as an estimator for CMP service life (Vilda, 2009). From the data collected, shown in Fig. 4.6, there was no correlation between resistivity and the deterioration rate of CMP. This is significant because electrical resistivity is commonly used to predict corrosion and has been for decades (Vilda, 2009).

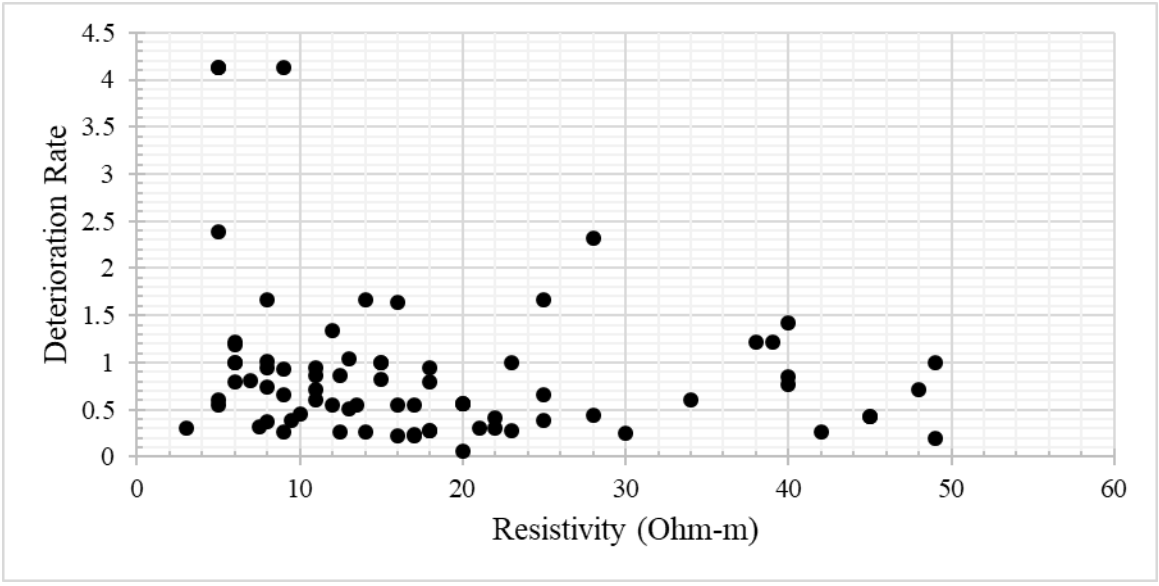

Fig. 4.6 Deterioration rate versus resistivity

The second property of the surrounding soil chosen for analysis was the chloride concentration present. This property was chosen because of small trial conducted by Crowder (2017) indicated there is possible correlation between the deterioration and chloride concentration. For this study, soil samples from eleven CMP were collected during the fall/winter before any snow had fallen. The initial chloride concentrations, extracted the day of collection, against the deterioration rate can be found in Fig. 4.7. With no consideration for outliers, the coefficient of determination was found to be 0.558. With the removal of the one apparent outlier of the initial chloride concentration of 2.42 ppm and deterioration rate of 3.33, the coefficient of determination rose to 0.881. Causes that may have led to outlying data were investigated including precipitation in the days prior to sample collection and observation and relative roadway traffic volume. However, no justification was found.

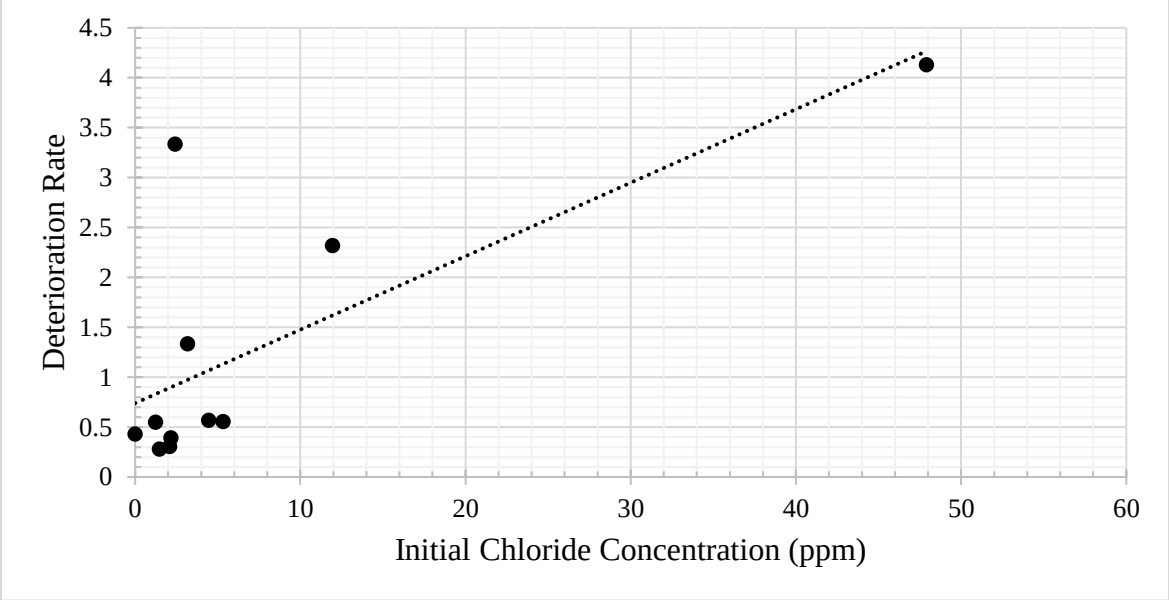

Fig. 4.7 Deterioration rate versus initial chloride concentration from CMP sampled in the fall/winter

Total chloride concentration was also measured against the deterioration rate. The resulting graph can be found in Fig. 4.8. The total chloride concentrations were calculated from

the chloride mobilized through repeated washing of the soil. With no consideration for outliers, the coefficient of determination was found to be 0.531. With the removal of the one apparent outlier, the same data point as previously described, the coefficient of determination rose to 0.826. From both the initial and total chloride concentration analyses, it can be concluded that chloride may be used as a good indicator of CMP deterioration rates in Kansas.

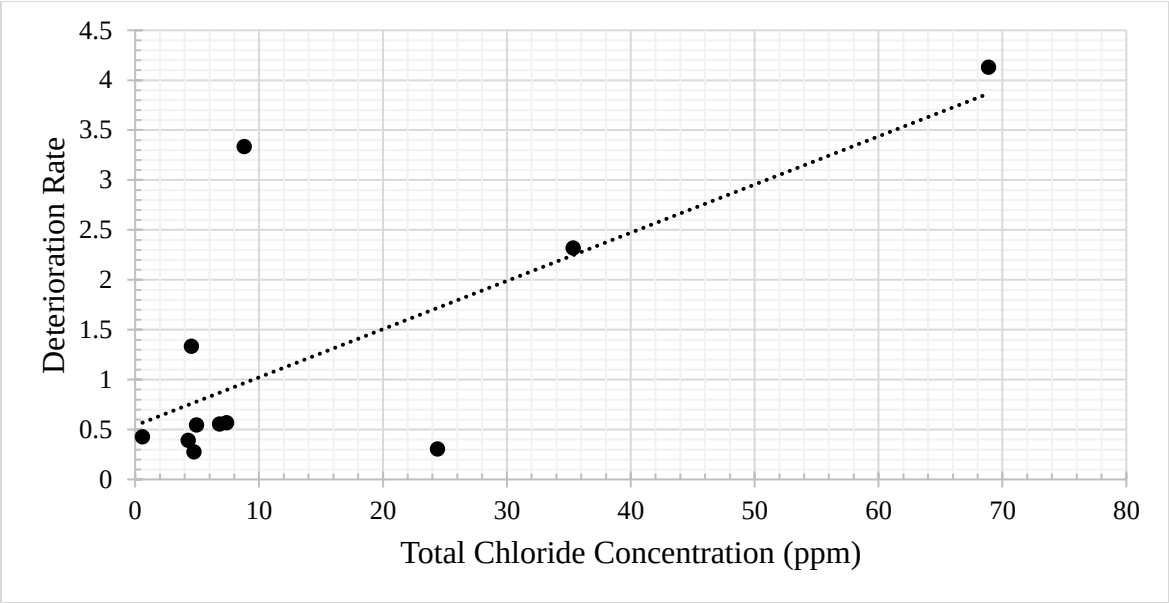

Fig. 4.8 Deterioration rate versus total chloride concentration from CMP sampled in the fall/winter

From the results of the chloride and resistivity analysis, it has been shown that resistivity is not a reliable indicator of CMP deterioration. On the other hand, chlorides were found to be an effective indicator of CMP deterioration. This findings of this study could potentially lead to a change in what soil properties are used and not used to predict CMP service life.

4.2.3 Summary

From the observation of 80 CMP in Kansas, it can be definitively concluded that the invert is of the most interest when assessing CMP corrosion due to its high variance and susceptibility to corrosion based on inadequate performance. This study confirmed the findings

of Stratton et al. (1990) that the policy change by KDOT in 1975, allowing for the installation of lighter gauge CMP, did have an adverse effect on the expected service life of the CMP installed after 1975 and before 1990. This study found that the reversion of the 1975 policy change did lower the deterioration rates of CMP closer to the pre-1975 levels. In addition to further investigating the conclusions of Stratton et al. (1990), this study examined the corrugation depth, CMP material, invert rating, deterioration rate, resistivity of the surrounding soil, and chloride concentration of the surrounding soil in an effort to find ways to better predict the deterioration rate of CMP. It was found that corrugation depth did not have any conclusive bearing on the invert rating of the two age groups examined. While there was not one material that performed the best in the two age groups that contained more than one material type, the traditional galvanized CMP did not perform the best in either category. Therefore it may be suitable to look towards aluminum and aluminized CMP for future installations. The resistivity, while commonly accepted as an indicator of corrosion, did not produce any trend when measured against the deterioration rate. The chloride concentration, on the other hand, did prove to be an indicator of the deterioration rate. This is especially true when considering previous work done by Crowder (2017) produced similar results.

4.3 MSE Walls

Five walls were analyzed for this research. All walls were tested with into-the-wall electrical resistivity arrays. Not every wall was tested with arrays at the top of the wall due to spatial and material constraints. The values for measured resistivity results at the top of the wall were capped at values lower than their absolute maximum in order more accurately visualize the results produced. The depth of investigation for the into-the-wall resistivity surveys were calculated for three array types: Schlumberger, Wenner, and Dipole-Dipole. These depths were

calculated using Edwards (1977) and Loke (1999). The other arrays did not have specified depth of investigations. The degree of saturation was calculated using Equation 3.2 and the accompanying assumptions.

4.3.1 Lee Blvd, Leawood, Kansas

The first wall investigated in this study was located at the Lee Blvd overpass of I-435 in Leawood, Kansas. This wall is adjacent to a park. This wall was topped with grass, allowing for top-of-the-wall surveys to be conducted. Both Dipole-Dipole and Schlumberger arrays were used at the top of the wall with electrode spacings of 0.5 m, 1 m, and 2 m in order to obtain a bulk characterization of the backfill and the soil underlying the MSE wall, as well as image the possible layer of fine soil particles collecting at the base of the wall. Both the Dipole-Dipole and Schlumberger arrays were used because of their different advantages. No Dipole-Dipole array with an electrode spacing of 2 m was used for analysis because of data collection error. Fig. 4.9 shows the results from the Dipole-Dipole array with a 0.5 m electrode spacing. The horizontal dotted line represents the base of the wall. The four vertical dotted lines represent the location of the four electrodes used for the into-the-wall survey. It shows a highly resistive material with a range of resistivity between 400 Ohm-m and 700 Ohm-m. This range of values is indicative of a gravel (Palacky, 1987).

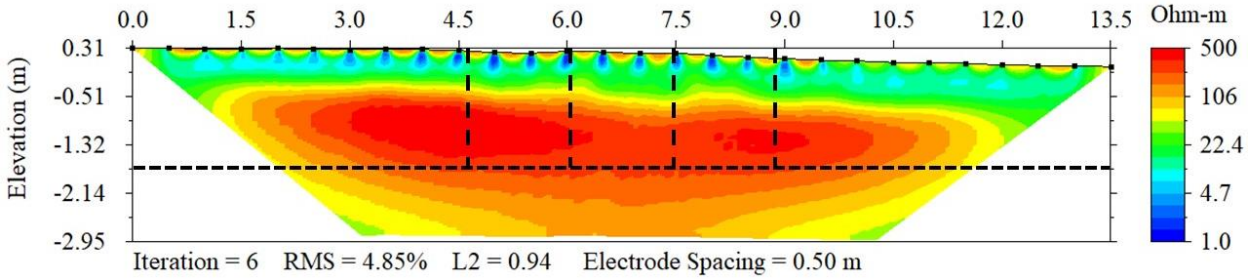

Fig. 4.9 Dipole-Dipole array with 0.5 m spacing at Lee Blvd, Leawood, Kansas

With a spacing of 1 m, the second Dipole-Dipole array, shown in Fig. 4.10, measured a similar, highly resistive material in the backfill of the MSE wall. Underlying the wall base (shown with the dashed line) is a material with a much lower resistivity between 35 Ohm-m and 50 Ohm-m. This is indicative of sandy clay. The two Dipole-Dipole surveys do not show a sharp interface between the backfill and the underlying soil.

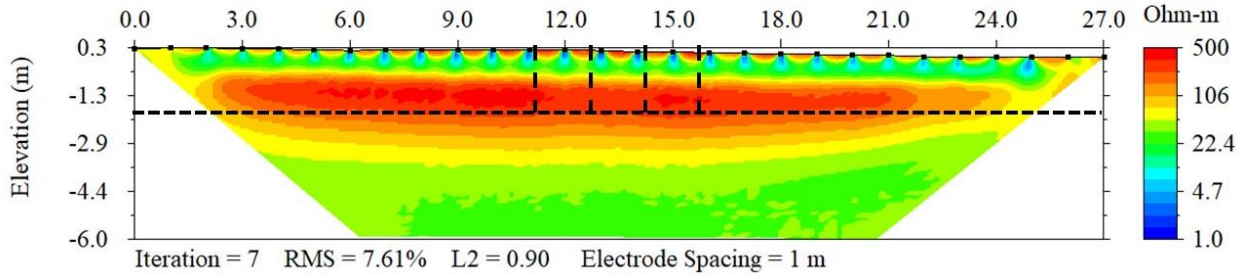

Fig. 4.10 Dipole-Dipole array with 1 m spacing at Lee Blvd, Leawood, Kansas

The results of the Schlumberger array performed at a spacing of 0.5 m, shown in Fig. 4.11, measured the backfill resistivity between 350 Ohm-m to 620 Ohm-m. This range of values for the backfill is comparable to those obtained by both of the Dipole-Dipole arrays. The backfill resistivity is indicative of gravel.

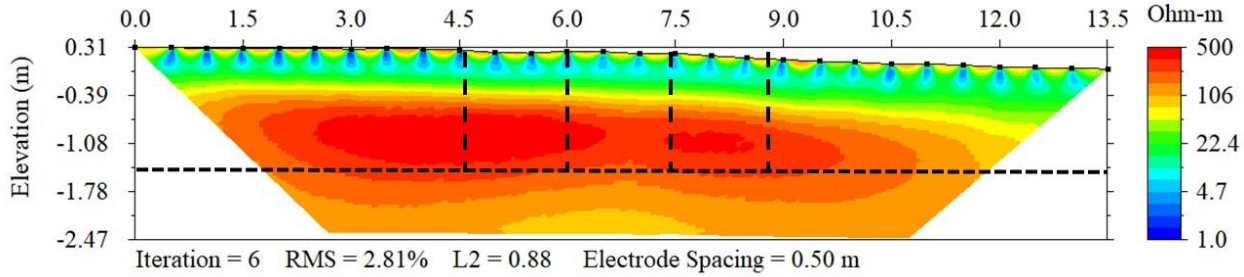

Fig. 4.11 Schlumberger array with 0.5 m spacing at Lee BLVD, Leawood, Kansas

Fig. 4.12 shows the results of the Schlumberger array taken with an electrode spacing of 1 m. The range in resistivity values for the backfill were 250 Ohm-m to 600 Ohm-m, again indicating gravel backfill. The lower end of the range was found at the base of the wall, indicating the possible presence of moisture in the backfill.

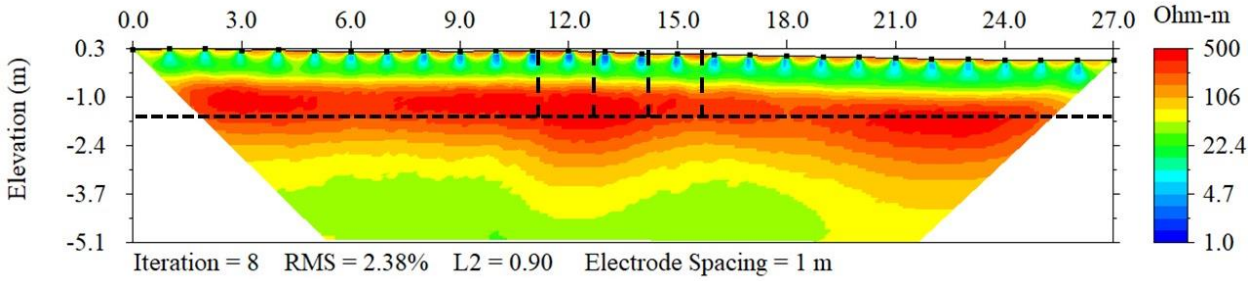

Fig. 4.12 Schlumberger array with 1 m spacing at Lee BLVD, Leawood, Kansas

The final electrical resistivity survey taken at this wall was a 2 m spaced Schlumberger array with the results displayed in Fig. 4.13. This survey was conducted to better image the soil underlying the wall. The resistivity of the underlying soil ranged from 60 Ohm-m to 50 Ohm-m. These relatively low values are indicative of sandy or silty clay with moisture.

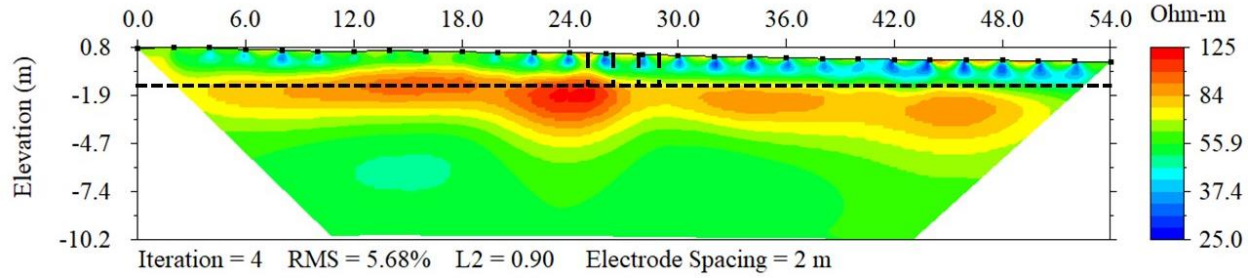

Fig. 4.13 Schlumberger array with 2 m spacing at Lee BLVD, Leawood Kansas

The results of the series of surveys taken into-the-wall can be found in Table 4.3. The electrode spacing for these surveys was 1.46 m and the total depth of investigation was no greater than 0.758 m behind the face of the wall. The depth of the backfill from the face of the wall, backwards, was approximately 1.25 m, or 0.7 times the height of the wall. With this electrode spacing, the depth of investigation for the into-the-wall surveys did not surpass the depth of the backfill behind the face of the wall. The resistivity measurements are lower than the values measured in any of the surveys from the top of the wall and are representative of wet

sand. Using Table 2.1, this backfill would be considered a moderately corrosive environment. The two merged array files are not provided because of data collection error.

Table 4.3 Into-the-wall resistivity at Lee BLVD, Leawood, Kansas

Array	Resistivity (Ohm-m)	Median Depth of Investigation (m)
Dipole-Dipole	25.1	0.607
Wenner	22.0	0.758
Schlumberger	21.7	0.758
Inverted Schlumberger	22.5	---

The classification of the MSE wall backfill collected at the base of the wall was poorly graded sand. The grain size distribution can be found in Fig. 4.14. It contained an *in situ* moisture content of 15.6%. The degree of saturation was calculated to be 51.7%. These laboratory tests are supportive of the into-the-wall measurements taken indicating wet sand. They also show that the surveys taken at the top of the wall were not effective at precisely revealing the conditions at the base of the wall. Neither array type or electrode spacing were more effective than the other in imaging the conditions at the base of the wall from a top survey. The resistivity of the backfill may have been increased due to the proximity of the survey to the wall face; being too close to the wall face will generate higher resistivity measurements (Snapp et al., 2017). However, these surveys were conducted at least one electrode spacing away from the wall face in order to neglect the effect of the wall face on the survey.

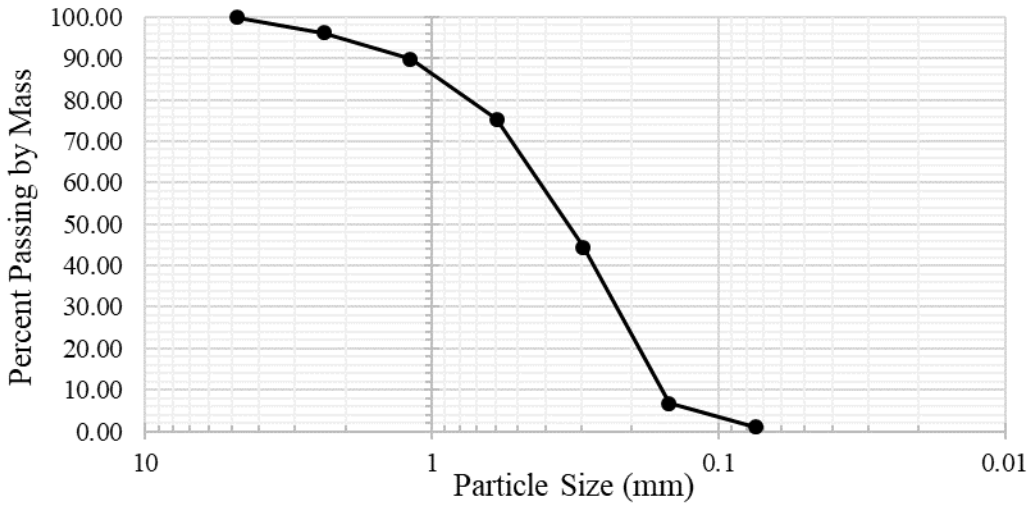

Fig. 4.14 Grain size distribution of MSE wall backfill at Lee Blvd, Leawood, Kansas

4.3.2 US-24 and Camp Creek Rd., Belvue, Kansas

The location of this MSE wall ran parallel to train tracks West of Belvue, Kansas. This wall showed many holes and channels that had formed directly behind the face of the wall. The severity of the one of the holes can be seen in Fig. 4.15.

Fig. 4.15 Hole in MSE wall at US-24 and Camp Creek Rd., Belvue Kansas

Without any prior knowledge it was expected that this wall would not have homogenous resistivity readings due to the loss of material and erosion. Because of the incline of this wall, only one survey was taken at the top of the wall. The results of the 1 m Dipole-Dipole are shown in Fig. 4.16. The results supported the predictions that the backfill would not produce homogenous results. Instead, the results show pockets of loose material in red and saturated pockets in blue.

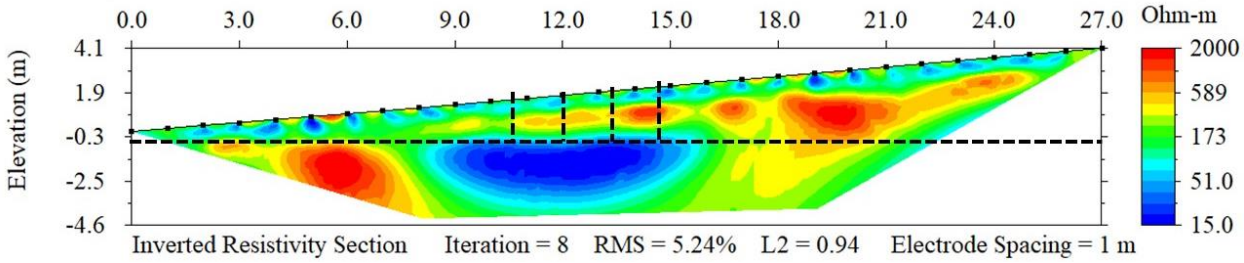

Fig. 4.16 Dipole-Dipole array with 1 m spacing at US-24 and Camp Creek Rd., Belvue, Kansas

The results of the into-the-wall survey can be found in Table 4.4. The electrode spacing was 1.5 m with a total depth of investigation of 1.558 m. The backfill depth was approximately 3.7 m at the sample location, confirming that the measurements only contained backfill material. The resistivity values are representative of sand with some moisture. Using Table 2.1, the backfill conditions would be considered non-corrosive. The into-the-wall resistivity data closely aligns with the survey data from the top-of-the-wall. However, this is misleading. It is most likely coincidental that the resistivity from both surveys match. The resistivity from the top-of-the-wall has been smoothed from the inversion process and does not depict the precise resistivity at that depth. Additionally, the reliability of the into-the-wall measurements are partially founded on the idea that the backfill is homogenous. This wall clearly has discontinuities behind the wall face and therefore show that the placement of the into-the-wall surveys have a large impact on the measurements taken. Had the into-the-wall measurements been taken 10 m to the

right of where they were originally taken, the resistivity measurements may have been much higher than what were actually taken.

Table 4.4 Into-the-wall resistivity at US-24 and Camp Creek Rd., Belvue, Kansas

Array	Resistivity (Ohm-m)	Median Depth of Investigation (m)
Dipole-Dipole	133.6	0.624
Wenner	118.0	0.779
Schlumberger	118.2	0.779
Inverted Schlumberger	117.7	---
Merged: Dipole-Dipole / Wenner	118.0 – 133.7	---
Merged: Dipole-Dipole / Schlumberger	118.2 – 133.7	---

The classification of the backfill was poorly graded sand with an *in situ* moisture content of 6.4%. The degree of saturation was calculated to be 21.2%. The grain size distribution can be found in Fig. 4.17. The findings from the laboratory tests are supportive of the into-the-wall measurements that were taken indicating sand with moisture. Compared to the MSE wall at Lee Blvd, the backfill had similar gradation but had a lower moisture content and degree of saturation. Additionally, the erosion of backfill causing heterogeneous air pockets that may exist where the survey was conducted would also increase the measured resistivity. The established relationship of saturation and resistivity supports the higher resistivity due to the lower moisture content. Air voids may have also influenced the increase in resistivity. Both sets of measurements are reasonable for their respective conditions.

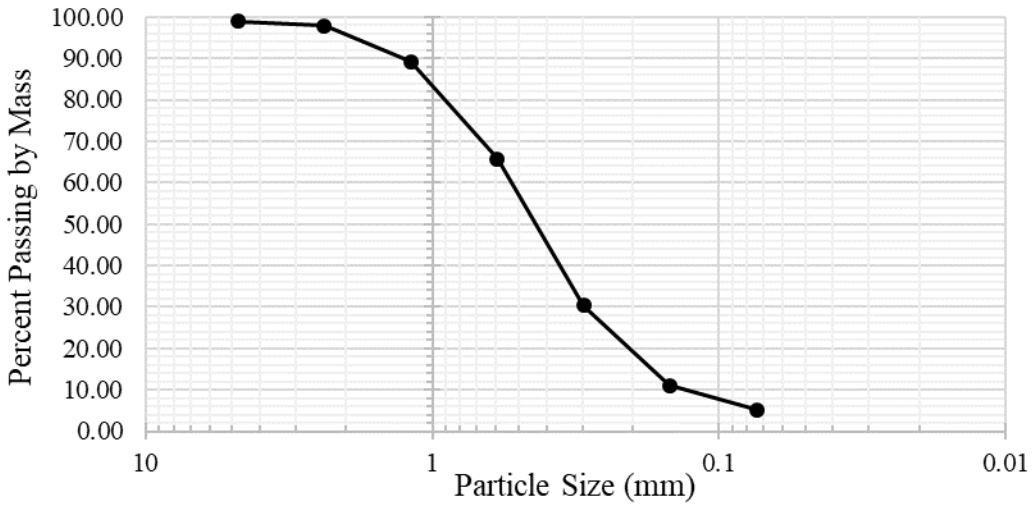

Fig. 4.17 Grain size distribution of MSE wall backfill at US-24 and Camp Creek Rd, Belvue, Kansas

4.3.3 US-75 and 46th St., Topeka, Kansas

The MSE wall found at US-75 and 46th St. is part of a bridge overpass. It had minimal access to the top of the wall, and what was accessible was covered in pavement. Therefore, no surveys were taken at the top of this wall. To this point, it has also been shown that the top-of-the-wall surveys do not clearly depict the conditions at the base of the walls. The electrical resistivity measurements taken into-the-wall are shown in Table 4.5. The electrode spacing was 2 m with a total depth of investigation of 2.076 m. The backfill depth was approximately 5.5 m, confirming that only backfill material resistivity was measured. The Dipole-Dipole array notwithstanding, these values are representative of wet sand. Using Table 2.1, the backfill environment would be considered moderately corrosive.

Table 4.5 Into-the-wall resistivity at US-75 and 46th St., Topeka, Kansas

Array	Resistivity (Ohm-m)	Depth of Investigation
Dipole-Dipole	334.9	0.832
Wenner	40.0	1.038
Schlumberger	39.9	1.038
Inverted Schlumberger	39.9	---
Merged: Dipole-Dipole / Wenner	39.9 – 337.1	---
Merged: Dipole-Dipole / Schlumberger	40.0 – 337.8	---

The classification of the backfill was poorly graded gravel. The calculated degree of saturation was 41.5%. The grain size distribution can be found in Fig. 4.18. The *in situ* moisture content was 4.7%. This classification does not support the into-the-wall measurements that predicted wet sand. Rather, this classification more reasonably supports the single Dipole-Dipole measurement which indicates gravel with some moisture. It would be beneficial to revisit this wall for a second analysis to get more consistent measurements. Each wall was only

available for into-the-wall testing once, so this wall could not be investigated further.

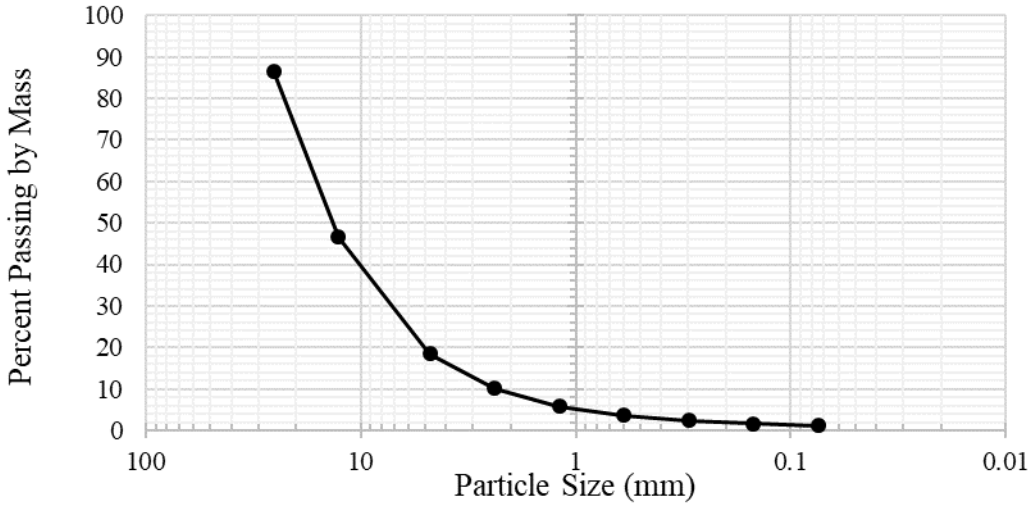

Fig. 4.18 Grain size distribution of MSE wall backfill at US-75 and 46th St., Topeka, Kansas

4.3.4 151st and I-35, Olathe, Kansas

The MSE wall located at 151st and I-35 was another wall incorporated into an overpass system. This one, however, was topped with soil and could be analyzed from the top as well as the bottom. The results from the top-of-the-wall survey can be seen in Fig. 4.19. The bulk resistivity of the backfill ranged from 150 Ohm-m to 400 Ohm-m, representing a slightly wet to dry sand. The underlying soil ranged from 5 Ohm-m to 35 Ohm-m representing a wet clay or the presence of a groundwater table.

Fig. 4.19 Dipole-Dipole array with 2 m spacing at 151st and I-35, Olathe, Kansas

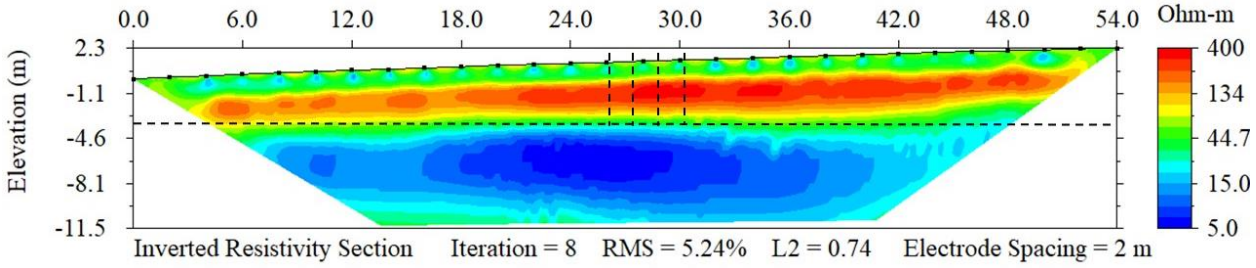

The results of the into-the-wall survey can be found in

Table 4.6. The electrode spacing was 1.55 m and the total depth of investigation was 1.608 m. The backfill depth was approximately 6 m at the testing location, indicating that the resistivity was measured only in the backfill. The resistivity measurements are indicative of a wet sand. Using Table 2.1, the backfill would be considered moderately corrosive at this depth. The top-of-the-wall survey appears to indicate similar resistivity to the into-the-wall survey. This is misleading. Rather, the resistivity shown at the base of the wall in the top-of-the-wall survey is due to smoothing from the inversion of the measured apparent resistivity between the backfill and the natural soil. Unfortunately, gradation data were not available yet to support the interpretation of the measurements into the face.

Table 4.6 Into-the-wall resistivity at 151st and I-35, Olathe, Kansas

Array	Resistivity (Ohm-m)	Depth of Investigation (m)
Dipole-Dipole	39.5	0.645
Wenner	46.6	0.804
Schlumberger	46.7	0.804
Inverted Schlumberger	45.3	---
Merged: Dipole-Dipole / Wenner	38.8 – 45.0	---
Merged: Dipole-Dipole / Schlumberger	38.7 – 44.9	---

4.3.5 K-10 and Ridgeview, Lenexa, Kansas

The MSE wall located at the intersection of K-10 and Ridgeview was topped with rip rap and could not be surveyed from the top. The results from the into-the-wall survey can be found in Table 4.7. The electrode spacing was 1 m and the total depth of investigation was 1.038 m.

The depth of the backfill was approximately 5.5 m and confirmed that the resistivity measurements only included the backfill. The resistivity measurements are representative of a moist sand or wet gravel. Using Table 2.1, the backfill at this depth would be considered non-corrosive.

Table 4.7 Into-the-wall resistivity at K-10 and Ridgeview, Lenexa, Kansas

Array	Resistivity (Ohm-m)	Depth of Investigation (m)
Dipole-Dipole	101.6	0.416
Wenner	101.4	0.519
Inverted Schlumberger	101.6	---

The classification of the backfill was poorly graded gravel with an *in situ* moisture content of 3.7%. The calculated degree of saturation was 32.7%. The grain size distribution can be found in Fig. 4.20. These results do not support the electrical resistivity measurements gathered. To match the gradation to the resistivity results, the moisture content should be higher or the measured resistivity should be higher.

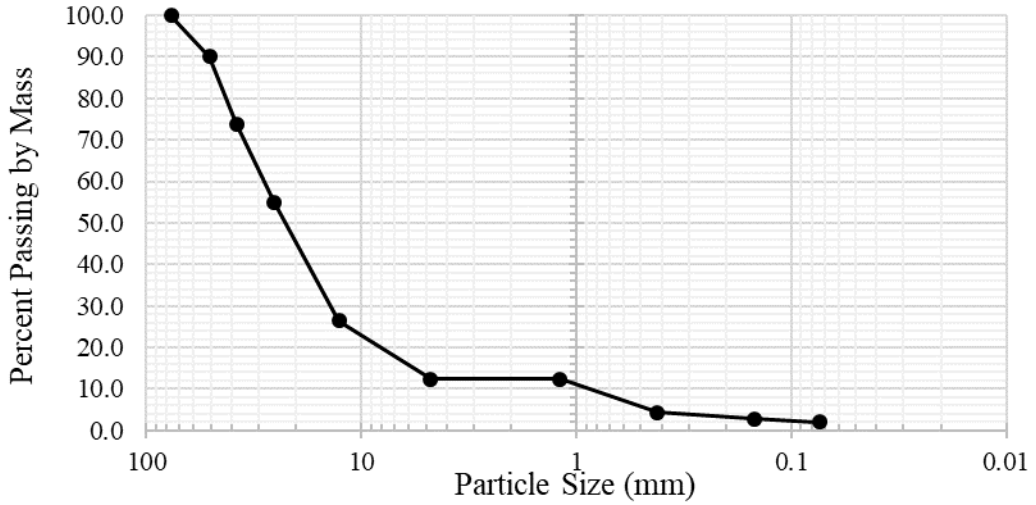

Fig. 4.20 Grain size distribution of MSE wall backfill at K-10 and Ridgeview, Lenexa, Kansas

Previous analysis on this wall was conducted by Snapp et al. (2017) and Brady et al. (2015). A gradation analysis showed the backfill contained over twice the amount of soil particles passing the 4.75 mm (No. 4) sieve than what was collected for the current study (Brady et al., 2015). This increase in small soil particles led to difficulties with laboratory testing conducted by Brady et al. (2015), specifically the testing apparatus did not drain well because of the presence of more small soil particles. The difference in gradation for what was the same wall exposed the limitations of the 2019 study. All of the backfill collected for analysis by the University of Kansas came from directly behind the face of the wall. Little to no backfill was able to be collected from more than 0.3 m from the wall face. This distance was not as far into the wall as the depth of investigation was for the resistivity surveys. The volume measured by resistivity but not collected for laboratory analysis could have contained more fine soil particles. This was in contrast to Brady et al. (2015) and Snapp et al. (2017) where backfill was able to be collected from the entire depth of backfill because it was collected during construction. It also showed that the backfill collected in the 2019 study did not completely reach the maximum depth of investigation of the into-the-wall surveys. For this wall in particular, the maximum depth of investigation was 0.519 m.

The resistivity of the backfill measured by KDOT at the time of construction was 60.36 Ohm-m. The resistivity was measured in accordance with AASHTO T 288. This value is much lower than the data collected from the into-the-wall surveys. However, Snapp et al. (2017) showed that AASHTO T 288 severely underestimates the resistivity of the backfill when compared to *in situ* measurements. The average measured *in situ* resistivity was 380.62 Ohm-m

(Snapp et al., 2017). Comparing this average measurement to the data found in Table 4.7, a large drop in resistivity in a relatively short amount of time is shown and should be a cause for concern for KDOT. The drop is likely due to an increase in moisture content or corrosion. However, this cannot be confirmed without destructive testing.

4.3.6 Summary

The use of electrical resistivity as a means to analyze MSE wall backfill provided mixed results. Two of the three top-of-the-wall surveys appeared to give accurate representations of the resistivity measured into-the-wall at the base. However, this was coincidental. Due to the nature of electrical resistivity and its data processing, electrical resistivity cannot be relied upon to give precise measurements at the desired subsurface location. The largest benefit of the top-of the-wall surveys is its ability to show discontinuities in backfill that would be missed with just a point measurement like the into-the-wall surveys. When able, the top-of-the-wall surveys should always be conducted to check for discontinuities.

The into-the-wall measurements showed promise in affirming the backfill type. The laboratory classification and classification based on resistivity can be found in Table 4.8. Only one of the five walls tested, located at K-10 and Ridgeview in Lenexa, KS, did not outright match the resistivity measurements to the gradation data. Two of the five walls, Lee Blvd in Leawood, KS and US-24 and Camp Creek Road in Belvue, KS, tested did match the resistivity measurements to the gradation data. The remaining two walls, US-75 and 46th St in Topeka, KS and 151st and I-35 in Olathe, KS, need further testing to validate or invalidate the resistivity measurements. The former would require another visit in the field to retest the into-the-wall resistivity, the latter is awaiting on the completion of laboratory testing. Assuming the backfill specifications are known prior to testing, the electrical resistivity measurements can identify if

moisture is present based on expected ranges of resistivity for different materials and moisture contents (Palacky, 1987 and Everett, 2013). Soils with similar gradation will have decreasing resistivity as moisture content increases. This fact was demonstrated by the Lee Blvd and US-24 and Camp Creek Rd MSE walls. Each of these walls had similar grain size distributions and were both classified as poorly graded gravel. The one with a higher moisture content (Lee Blvd) had lower into-the-wall resistivity measurements than the other. The same trend persists with the degree of saturation, which is partially reliant on the moisture content. The degree of saturation for Lee Blvd was 51.7% and for Camp Creek Rd was 21.2%. Comparing the degree of saturation to one another can be more effective than moisture content at portraying the difference in water present because the in numbers is greater in the degree of saturation. The degree of saturation measures volume of water in relation to the void space while the moisture content measures the volume of water in relation to the volume of the void space and solid matrix.

Additionally, these measurements can identify corrosive environments (Elias et al., 2009). Two walls, Lee Blvd and 151st and I-35, were assessed as moderately corrosive environments. Two other walls, US-24 and Camp Creek Rd and K-10 and Ridgeview, were assessed as non-corrosive. The remaining wall's resistivity data spanned multiple levels of corrosion aggression and should be retested to validate or correct the data. Note that while the Ridgeview data did not support gradation the low resistivity may have been caused by corrosion that has already taken place. This was not confirmed and was outside the scope of this research. Rather, the purpose of this research was to indicate corrosive environments in MSE wall backfill.

Table 4.8 Laboratory and into-the-wall resistivity data

Street	Top Cover	Classification (Lab)	Moisture Content (%)	Saturation (%)	Classification (Resistivity)	Field Resistivity (Ohms)	
						Min	Max
Lee Blvd	Soil	Poorly Graded Sand	15.6	51.7	Wet Sand	21.7	25.1
US-24 & Camp Creek Rd	Soil	Poorly Graded Sand	6.4	21.2	Moist Sand	117.7	133.7
US-75 & 46th St	Pavement	Poorly Graded Gravel	4.7	41.5	???	39.9	337.8
151st & I-35	Soil	---	---	---	Wet Sand	38.7	46.7
K-10 and Ridgeview	Rip-Rap	Poorly Graded Gravel	3.7	32.7	Moist Gravel	101.4	101.6

While this study did not investigate the corrosion of the metallic reinforcing strips in the MSE walls, walls with lower into-the-wall electrical resistivity measurements had more corrosion potential based on Table 2.1. The drawback of the into-the-wall measurements are that they can be misleading. These measurements operate with the assumption that the backfill is homogenous and results in Fig. 4.16 show that is not always the case. With only the into-the-wall measurements, the MSE wall at US-24 and Camp Creek Rd. would have been passed over as a non-corrosive environment and some of the larger structural concerns could have been missed. Therefore, into-the-wall electrical resistivity surveys are very dependent on the location of the measurements. The comparison of different studies on the same wall at K-10 and Ridgeview showed the importance of initial measurements. Knowing the resistivity of the backfill at installation allows KDOT to see how rapidly the conditions within the backfill are

deteriorating. In the case of this MSE wall, the conditions seem to be deteriorating rapidly. Therefore, if used for monitoring, a drop in resistivity from the initial measurement would indicate the existence of a corrosive environment resulting from the presence of fine soil particles, water, and/or dissolved salts. A drop in resistivity could also indicate that corrosion has already occurred.

Chapter 5 - Conclusions and Future Work

5.1 Conclusions

The deterioration rate of CMP was weighed against many material and soil properties in an effort to better understand the corrosion of CMP in Kansas. This research found that CMP was most vulnerable when it was a lighter gauge and had higher chloride concentrations in the surrounding soil. Properties such as corrugation depth and material type did not have a clear influence on the invert rating. Contrary to common practice, the resistivity was not a useful indicator of deterioration rate because there was no correlation.

The assessment of MSE wall backfill using electrical resistivity provided mixed results. The top-of-the-wall surveys did not aid in the validation of the into-the-wall measurements, but those surveys still served a purpose. The top of the wall surveys indicated abnormalities in the backfill and can be used to help direct the placement of into-the-wall surveys. The into-the-wall surveys were varied. Two walls accurately represented the gradation and moisture content, while one did not. The remaining two walls were inconclusive and would benefit from further testing. All measurements were limited to a single testing opportunity.

5.2 Future Work

Future work regarding the observation of aluminum and aluminized CMP is appropriate. Because these materials were barred from use in Kansas before 2001, it would be interesting to see how these CMP fare 30 or more years after installation. Also, because of the relative newness of these pipes, fewer existed for analysis. It would be beneficial to add more aluminum and aluminized CMP to these results to further strengthen the conclusions made.

Additionally, the analysis of chloride concentrations in the soil surrounding CMP during different months would prove valuable when assessing deterioration rates of CMP. A number of

variables could be investigated. One of those variables is the effects of rainfall or lack of rainfall in the days prior to soil collection. Another variable of interest would be the influence of road deicers and their immediate and long term influence. It is known that road deicers increase the salt concentration in roadside ditches (Wilmert et al, 2018) after application, but the length of time these dissolved salts remain in the soil is variable. With an improved understanding of the effects of rainfall and deicers on ion concentrations in the roadside soil, an appropriate time to sample soils surrounding CMP for the prediction of corrosion could be more appropriately determined.

Pertaining to the study of corrosive environments in MSE walls, future studies could examine the change in MSE wall backfill resistivity over time. Establishing baseline resistivity for MSE walls would be beneficial for comparing the resistivity measurements taken at a later date, similar to the measurements in this study. The change in resistivity from the baseline to the future measurements could show the development of a corrosive environment in the backfill, or show no development of such an environment. With no knowledge of the initial resistivity, this study could not say to what degree had the backfill environment changed and how much more susceptible to corrosion the metallic reinforcing strips were now compared to installation.

Other backfill properties could be measured in addition to resistivity. A list of properties that could be of interest are the pH, organic content, and sulfates. Utilizing those would ensure that a baseline measurement is acquired for future reference. Regarding the concentration of chlorides, this thesis showed that the concentration of chlorides in soil were a better predictor of the deterioration rate in CMP than resistivity. It is possible that these findings are consistent with other roadside metallic elements, such as MSE wall reinforcement.

Chapter 6 - References

AASHTO. (2012). Standard method of test for determining minimum laboratory soil resisitivty. Washington, D.C.: American Association of State Highway and Transportation Officials.

AGI (Advanced Geosciences, Inc.). (2008). Instruction Manual for EarthImager 2D Version 2.4.0 Resistivity and IP Inversion Software. Advanced Geosciences, Inc., Austin, TX.

Ahmad, Zaki. (2006). Principles of corrosion engineering and corrosion control. Elsevier Science & Technology.

Armour, T., Bickford, J., & Pfister, T. (2004). Repair of failing MSE railroad bridge abutment. In J.P. Turner & P.W. Mayne (Eds.), GeoSupport 2004: Drilled Shafts, Micropiling, Deep Mixing, Remedial Methods, and Specialty Foundation Systems (pp. 380-394). Reston, VA: American Society of Civil Engineers.

Averill, B., & Eldredge, P. (2012). General Chemistry: Principles, Patterns, and Applications. Saylor Foundation.

ASTM International. (2012a). ASTM G57-06(2012) Standard test method for field measurement of soil resistivity using the Wenner four-point electrode method. West Conshohocken, PA: ASTM International.

ASTM International. (2012b). ASTM NACE/ASTMG193-12d Standard terminology and acronyms relating to corrosion. West Conshohocken, PA: ASTM International.

ASTM International. (2012c). ASTM G187-12a Standard test method for measurement of soil resistivity using the two-electrode soil box method. West Conshohocken, PA: ASTM International.

ASTM International (2017). ASTM D2487-17 Standard practice for classification of soils for engineering purposes (unified soil classification system). West Conchohocken, PA: ASTM International.

Brady, Z., Parsons, R., & Han, J. (2015). Testing aggregate backfill for corrosion potential. Technical Report No. K-TRAN: KU-15-5. Kansas Department of Transportation

CALTRANS. (1999) Method for estimating the service life of steel culverts. California Department of Transportation, Sacramento, California.

Cicek, V. (2014) Corrosion Engineering. John Wiley & Sons, New York.

Crowder, Andrew N. (2017). Field and laboratory characterization of corrosion potential in highway corrugated metal pipe. Kansas State University.

DeSimone, L. A., McMahon, P. B., & Rosen, M. R. (2014). Water quality in principal aquifers of the United States, 1991-2010. United States Geological Survey, Circular 1360.

Edwards, L. S. (1977). A modified pseudosection for resistivity and IP. Geophysics, 42(5), 1020-1036.

Elias, V., Fishman, K.L., Christopher, B.R., & Berg, R.R. (2009). Corrosion/degradation of soil reinforcements for mechanically stabilized earth walls and reinforced soil slopes (Report No. FHWA-NHI-09-087). Washington, DC: Federal Highway Administration.

Everett, M. E. (2013) Near-Surface Applied Geophysics. Cambridge University Press, New York, NY. 4, 70-102.

Gerber, T. M., & Billings, D. A., (2010). Assessing corrosion of MSE wall reinforcement. Research Division, Report No. UT-10.20. Utah Department of Transportation.

Hageman, P. L. (2007). U.S. Geological survey field leach test for assessing water reactivity and leaching potential of mine wastes, soils, and other geologic and environmental materials. US Geological Survey Techniques and Methods, 5(D3), 1-14.

Hallof, Philip. (1957). On the interpretation resistivity and induced polarization field results. Cambridge, MIT. Ph.D. Thesis.

Hansen, Justin. (2015). Aggregates for backfill. Materials Division. Kansas Department of Transportation, Section 1107.

Herb, William. (2017). Study of de-icing salt accumulation and transport through a watershed. Minnesota Department of Transportation.

Holtz, R. D., Kovacs, W. D., & Sheahan, T. C. (2011). An introduction to geotechnical engineering. Second Edition. Pearson Education, Inc.

Kutz, Myer. (2005). Handbook of environmental degradation of materials. William Andrew Publishing.

Li, F., Zhang, Y., Fan, Z., & Oh. K. (2015) Accumulation of de-icing salts and its short-term effect on metal mobility in urban roadside soils. Bulletin of Environmental Contamination and Toxicology, 94(4), 525-531.

Loke, M. H. (1999). Electrical imaging sruveys for environmental engineering studies: a practical guide to 2-D and 3-D surveys.

Palacky, G. (1987). Resistivity characteristics of geological targets, in electromagnetic methods in applied geophysics, edited by Misac Nabighian, Society of Exploration Geophysicists. Society of Exploration Geophysicists, 1, 55.

Sawin, R. S., & Buchanan, R. C. (2002). Salt in Kansas. Kansas Geological Survey, Public Information Circular, 21.

Snapp, M., Tucker-Kulesza, S., & Koehn, W. (2017). Electrical resistivity of mechanically stabilized earth wall backfill. Journal of Applied Geophysics, 141, 98-106.

Stratton, W. (1989). Corrugated metal pipe culvert performance final report. Bureau of Materials and Research. Kansas Department of Transportation.

Stratton, F. W., Frantzen, J. A., & Meggers, D. A. (1990). Cause of accelerated deterioration of corrugated metal pipe installed after 1974. Bureau of Materials and Research, Technical Report No. KS-90/3. Kansas Department of Transportation.

Thornley, J. D., and Siddharthan, R. V. (2010). "Effects of corrosion aggressiveness on MSE wall stability in Nevada." Proc., 2010 Earth Retention Conference, American Society of Civil Engineers, Bellevue, Washington, 539-547.

Tucker-Kulesza, S., Snapp, M., & Koehn, W. (2016). Electrical resistivity measurement of mechanically stabilized earth wall backfill. Technical Report No. K-Tran: KSU-15-6. Kansas Department of Transportation.

United States Geological Survey, (2018). Saline Water and Salinity. Retrieved from: https://www.usgs.gov/special-topic/water-science-school/science/saline-water-and-salinity?qt-science_center_objects=0#qt-science_center_objects

Urrea, G. J. C. (2014). Service life of concrete and metal culverts located in Ohio Department of Transportation districts 9 and 10. Russ College of Engineering and Technology.

Vilda, W. S. (2009). Corrosion in the soil environment: soil resistivity and pH measurements. National Cooperative Highway Research Program. Transportation Research Board, National Research Council.

Virmani, Y. P., Payer, J. H., Koch, G. H., Brongers, M. P. H., Thompson, N. G. (2002). Corrosion costs and preventative strategies in the United States. Federal Highway Administration, Publication No. FHWA-RD-01-156.

Wilmert, H. M., Osso. J. D., Twiss, M. R., Langen, T. A., (2018) Winter road management effects on roadside soil and vegetation along a mountain pass in the Adirondack Park, New York, USA. Journal of Environmental Management, 225, 215-223.

Appendix A - 2018 CMP Data Sets

Table A.1 Summary of all CMP surveyed in 2018

ID	Project/Route Number	County	Material	Age (yrs)	Diameter (in)	Pitch (in)	Depth (in)	Description
3	K-18	Riley	Aluminized	7	18	2.67	0.5	5 inches of sediment
4	K-18	Riley	Aluminized	7	18	2.67	0.5	5 inches of sediment
5	K-18	Riley	Aluminized	7	18	2.67	0.5	3.5 inches of sediment
6	K-18	Riley	Aluminized	7	18	2.67	0.5	10 inches of sediment
7	K-18	Riley	Aluminized	7	18	2.67	0.5	10 inches of sediment
14	99 C-4549-01	Wabaunsee	Aluminum	7	18	2.67	0.5	10 in of sediment
59	US-75	Osage	Aluminum	7	30	2.67	0.5	
60	US-75	Osage	Aluminum	7	30	2.67	0.5	
35	C-143	Johnson	Aluminum	9	36	2.67	0.5	
32	US-56	Johnson	Aluminum	9	60	3.00	1	standing water
15	Hodges Rd	Shawnee	Aluminum	11	24	2.67	0.5	17 in of sediment; could not locate Side A
85	K-18	Riley	Aluminized	12	18	2.67	0.5	could not locate Side A
16	SW 53rd St	Shawnee	Aluminized	13	18	2.67	0.5	Side B overgrown
26	23 C-3472-01	Douglas	Galvanized	15	48	2.67	0.5	standing water
27	23 C-3472-01	Douglas	Galvanized	15	48	2.67	0.5	standing water
22	23 U-1749-01	Douglas	Galvanized	16	12	2.67	0.5	could not locate Side A
61	K-31	Osage	Galvanized	16	24	2.67	0.5	3 inches of sediment
70	43 C-3770-01	Jackson	Galvanized	16	24	2.67	0.5	could not locate Side B
71	43 C-3770-01	Jackson	Galvanized	16	24	2.67	0.5	could not locate Side A
40	I-70	Shawnee	Galvanized	16	30	2.67	0.5	could not locate Side A

34	C-199	Johnson	Aluminum	17	18	2.67	0.5	Side B overgrown
68	US-75	Shawnee	Aluminum	18	15	2.67	0.5	standing water; could not locate Side B
69	US-75	Shawnee	Aluminum	18	18	2.67	0.5	standing water; could not locate Side B
38	99 C-3459-01	Wabaunsee	Galvanized	18	18	2.67	0.5	
36	99 C-3459-01	Wabaunsee	Galvanized	18	24	2.67	0.5	
37	99 C-3459-01	Wabaunsee	Galvanized	18	24	2.67	0.5	
72	44 C-2271-01	Jefferson	Galvanized	19	18	2.67	0.5	
84	56 C-3586-01	Lyon	Galvanized	19	18	2.67	0.5	could not locate Side B
18	10-23 K-3359-04	Douglas	Galvanized	21	24	2.67	0.5	
20	10-23 K-3359-04	Douglas	Galvanized	21	24	2.67	0.5	bituminous coating
21	10-23 K-3359-04	Douglas	Galvanized	21	24	2.67	0.5	
39	99 C-1982	Wabaunsee	Galvanized	22	24	2.67	0.5	5 in of sediment
23	10-23 K-3359-03	Douglas	Galvanized	22	48	2.67	0.5	24 in sediment; standing water - no invert rating
31	169-46K-5343-01	Johnson	Galvanized	23	24	2.67	0.5	Side A overgrown
25	10-23 K-3359-10	Douglas	Galvanized	23	36	2.67	0.5	
29	169-46K-5343-01	Johnson	Galvanized	23	48	2.67	0.5	standing water
30	169-46K-5354-01	Johnson	Galvanized	23	48	2.67	0.5	standing water
33	56-46 K-2643-01	Johnson	Galvanized	24	30	2.67	0.5	
28	K-7	Wyandotte	Galvanized	35	36	2.67	0.5	
53	US-36	Brown	Galvanized	41	42	2.67	0.5	
54	US-36	Brown	Galvanized	41	42	2.67	0.5	
50	US-36	Brown	Galvanized	41	48	2.67	0.5	
49	US-36	Brown	Galvanized	41	54	3.00	1	
52	US-36	Brown	Galvanized	41	60	3.00	1	
46	US-36	Brown	Galvanized	41	72	3.00	1	

47	US-36	Brown	Galvanized	41	72	3.00	1	invert covered in concrete
48	US-36	Brown	Galvanized	41	72	3.00	1	
1	K-16	Pottawatomie	Galvanized	53	36	2.67	0.5	7 inches of sediment
2	K-16	Potawattomie	Galvanized	53	36	2.67	0.5	7 inches of sediment
77	US-59	Allen	Galvanized	58	24	2.67	0.5	standing water
78	US-59	Allen	Galvanized	58	24	2.67	0.5	4 inches of sediment
79	US-59	Allen	Galvanized	58	24	2.67	0.5	
80	US-59	Allen	Galvanized	58	24	2.67	0.5	3 inches of sediment
81	US-59	Allen	Galvanized	58	24	2.67	0.5	4 inches of sediment
45	US-36	Nemaha	Galvanized	60	42	2.67	0.5	standing water
55	Old 75	Shawnee	Galvanized	61	24	2.67	0.5	14 in of sediment
8	K-99	Wabaunsee	Galvanized	64	24	2.67	0.5	
9	K-99	Wabaunsee	Galvanized	64	24	2.67	0.5	11 inches of sediment
10	K-99	Wabaunsee	Galvanized	64	30	2.67	0.5	6 in of sediment
12	K-99	Wabaunsee	Galvanized	64	30	2.67	0.5	16 in sediment
13	K-99	Wabaunsee	Galvanized	64	30	2.67	0.5	10 in of sediment
11	K-99	Wabaunsee	Galvanized	64	48	3.00	1	6 in of sediment
89	K-9	Sheridan	Aluminized	65	36	2.67	0.5	Long-term study, standing water
73	K-192	Jefferson	Galvanized	67	18	2.67	0.5	
74	K-192	Jefferson	Galvanized	67	18	2.67	0.5	
75	K-192	Jefferson	Galvanized	67	36	2.67	0.5	standing water
57	Old 75	Shawnee	Galvanized	69	18	2.67	0.5	
58	Old 75	Shawnee	Galvanized	69	24	2.67	0.5	4 in sediment
56	Old 75	Shawnee	Galvanized	69	30	2.67	0.5	
41	K-63	Pottawatomie	Galvanized	80	18	2.67	0.5	

42	K-63	Pottawatomie	Galvanized	80	24	2.67	0.5	
44	K-63	Pottawatomie	Galvanized	80	24	2.67	0.5	
86	K-63	Pottawatomie	Galvanized	80	24	2.67	0.5	
43	K-63	Pottawatomie	Galvanized	80	36	2.67	0.5	
62	K-170	Osage	Galvanized	82	24	2.67	0.5	6 inches of sediment
63	K-170	Osage	Galvanized	82	24	2.67	0.5	standing water
64	K-170	Osage	Galvanized	82	24	2.67	0.5	standing water; could not locate Side B
65	US-56	Osage	Galvanized	88	60	5.00	1	standing water
66	US-56	Osage	Galvanized	88	60	5.00	1	standing water
67	US-56	Osage	Galvanized	88	60	5.00	1	standing water

Table A.2 Ratings of CMP surveyed in 2018

ID	General Condition (A)	External A	Crown A	Side A	Invert A	General Condition (B)	External B	Crown B	Side B	Invert B	Resistivity
3	88.5	88	90	88	88	88.5	88	90	88	88	1500
4	88.5	88	90	88	88	88.5	88	90	88	88	1500
5	91	92	92	90	90	91	92	92	90	90	4800
6	92	92	92	92	92	92	92	92	92	92	4500
7	92	92	92	92	92	92	92	92	92	92	4500
14	82.5	60	90	90	90	82.5	60	90	90	90	1100
59	88	88	88	88	88	88	88	88	88	88	600
60	93.25	95	95	95	88	93.25	95	95	95	88	600
35	93.75	95	95	95	90	93.75	95	95	95	90	1200
32	42.5	0	85	85	0	93.75	95	95	95	90	500
15	null	null	null	null	null	90	90	90	90	90	1000
85	null	null	null	null	null	94.25	95	95	95	92	3000
16	90.5	90	90	92	90	null	null	null	null	null	2500
26	86.5	92	92	92	70	80.25	92	92	92	45	1400
27	86	92	92	92	70	86	92	92	92	70	2500
22	null	null	null	null	null	77.25	45	92	92	80	1800
61	90	90	90	90	90	90	90	90	90	90	750
70	90	90	90	90	90	null	null	null	null	null	2100
71	null	null	null	null	null	91	92	92	90	90	2200
40	null	null	null	null	null	84.5	85	85	88	80	900
34	91.5	95	95	88	88	null	null	null	null	null	2200
68	92	92	92	92	null	null	null	null	null	null	600

69	79.25	92	90	90	45	null	null	null	null	null	900
38	90.5	92	90	90	90	90.5	92	90	90	90	2300
36	90	90	90	90	90	90	90	90	90	90	1800
37	90	90	90	90	90	90	90	90	90	90	1800
72	90	90	90	90	90	90	90	90	90	90	4200
84	89	92	92	92	80	null	null	null	null	null	1800
18	86.5	92	92	92	70	86.5	92	92	92	70	600
20	82	88	90	90	60	82	88	90	90	60	800
21	70.5	95	92	92	0	81.75	95	92	92	45	500
39	90	90	90	90	90	90	90	90	90	90	1700
23	null	92	92	70	null	null	92	92	70	null	2000
31	null	null	null	null	null	69	92	92	92	0	900
25	80.25	92	92	92	45	89	92	92	92	80	2500
29	60	60	92	88	0	68	92	92	88	0	500
30	69	92	92	92	0	69	92	92	92	0	500
33	86.5	92	92	92	70	86.5	92	92	92	70	1300
28	85.5	70	92	92	88	85.5	70	92	92	88	4900
53	66.25	85	90	90	0	78.75	90	90	90	45	3900
54	82	88	90	90	60	72.5	90	90	80	30	4000
50	67.5	90	90	90	0	66.25	85	90	90	0	2800
49	67.5	90	90	90	0	76.25	45	90	90	70	3400
52	78.75	90	90	90	45	67.5	90	90	90	0	3800
46	78.75	90	90	90	45	62.5	70	90	90	0	600
47	null	90	90	90	null	null	45	90	90	null	600
48	67.5	90	90	90	0	80	70	90	90	70	1100

1	75	80	90	85	45	75	80	90	85	45	800
2	80	80	90	90	60	80	80	90	90	60	900
77	78.75	90	90	90	45	78.75	90	90	90	45	1250
78	78.75	90	90	90	45	78.75	90	90	90	45	1100
79	85	80	90	90	80	82.5	80	90	80	80	1400
80	87.5	90	90	90	80	65	0	90	90	80	1250
81	62.5	70	90	90	0	62.5	70	90	90	0	1600
45	71.25	90	90	90	15	71.25	90	90	90	15	1200
55	72.5	80	85	80	45	72.5	80	85	80	45	1500
8	85	90	90	90	70	85	90	90	90	70	950
9	87	88	90	90	80	78.25	88	90	90	45	1700
10	60	60	60	60	60	60	60	60	60	60	1350
12	67	60	90	88	30	67	60	90	88	30	800
13	76	60	92	92	60	76	60	92	92	60	1600
11	61.25	45	70	70	60	61.25	45	70	70	60	1700
89	76.25	90	90	80	45	75.75	88	90	80	45	4000
73	68.25	70	88	70	45	68.25	70	88	70	45	800
74	77.5	85	85	70	70	35	0	0	70	70	800
75	63.75	85	85	85	0	63.75	85	85	85	0	4000
57	79.5	88	85	85	60	79.5	88	85	85	60	1300
58	40	0	85	45	30	40	0	85	45	30	1100
56	82.5	80	85	85	80	62.5	80	85	85	0	1600
41	58.75	45	70	60	60	58.75	45	70	60	60	2800
42	66.25	80	85	85	15	66.25	80	85	85	15	2300
44	62.5	80	85	85	0	70	80	85	85	30	700

86	68.75	80	90	90	15	68.75	80	90	90	15	4900
43	72.5	80	90	90	30	90	90	90	90	90	2000
62	72	88	85	85	30	36.25	0	30	85	30	600
63	70	80	80	60	60	80	80	85	85	70	300
64	58.75	70	60	60	45	null	null	null	null	null	500
65	68.75	85	85	60	45	68.75	85	85	60	45	2000
66	62.5	85	60	60	45	62.5	85	60	60	45	2000
67	75	85	85	85	45	65	85	85	45	45	2000

Appendix B - MSE Wall Information

Table B.1 MSE Wall Specifications

Street	Top Cover	Reinforcement Type	Classification (Lab)	USCS Classification	Moisture Content (%)	Saturation (%)	Classification (Resistivity)	Field Resistivity (Ohms)	
								Min.	Max.
Lee Blvd	Soil	Metallic	Poorly Graded Sand	SP	15.6	51.7	Wet Sand	21.7	25.1
US-24 & Camp Creek Rd	Soil	Metallic	Poorly Graded Sand	SP	6.4	21.2	Moist Sand	117.7	133.7
US-75 & 46th St	Pavement	Metallic	Poorly Graded Gravel	GP	4.7	41.5	???	39.9	337.8
151st & I-35	Soil	Metallic	---	---	---	---	Wet Sand	38.7	46.7
K-10 and Ridgeview	Rip-Rap	Metallic	Poorly Graded Gravel	GP	3.7	32.7	Moist Gravel	101.4	101.6
SB Antioch to I-435 WB	Rip-Rap	Metallic	---	---	---	---	Dry Gravel	631.9	725.0
I-435 to Lackman/I-35 SB	Soil	Metallic	---	---	---	---	Wet Sand	83.0	88.1
I-135 & W. Magnolia Rd.	Pavement	Metallic	---	---	---	---	Wet Sand	46.6	68.0

Table B.2 MSE Wall Resistivity Measurements

Street	City	Dipole-Dipole	Wenner	Schlumberger	Inverted Schlumberger	Merged: Dipole-Dipole / Wenner	Merged: Dipole Dipole / Schlumberger
Lee Blvd	Leawood	25.1	22.0	21.7	22.5	---	---
US-24 & Camp Creek Rd	Belvue	133.6	118.0	118.2	117.7	118.0 - 133.7	118.2 - 133.7
US-75 & 46th St	Topeka	334.9	40.0	39.9	39.9	39.9 - 337.1	40.0 - 337.8
151st & I-35	Olathe	39.5	46.6	46.7	45.3	38.8 - 45.0	38.7 - 44.9
K-10 and Ridgeview	Lenexa	101.6	101.4	---	101.6	---	---
SB Antioch to I-435 WB	Olathe	722.3	634.3	634.4	631.9	641.0 - 725.0	640.0 - 717.0
I-435 to Lackman/I-35 SB	Lenexa	83.0	87.3	87.1	88.1	83.3 - 87.0	83.1 - 87.1
I-135 & W. Magnolia Rd.	Salina	67.3	47.5	47.8	47.0	46.7 - 68.0	46.6 - 68.0